BCSJ

Vol. 90 Commemorative Account: Self-Organization

Two-Dimensional (2D) Nanomaterials towards Electrochemical Nanoarchitectonics in Energy-Related Applications

Ali Hossain Khan,[1] Srabanti Ghosh,[1] Bapi Pradhan,[1] Amit Dalui,[1,2] Lok Kumar Shrestha,*[2] Somobrata Acharya,*[1] and Katsuhiko Ariga*[2,3]

[1]Centre for Advanced Materials, Indian Association for the Cultivation of Science, Jadavpur, Kolkata 700032, India

[2]World Premier International Center for Materials Nanoarchitectonics (WPI-MANA), National Institute for Materials Science (NIMS), 1-1 Namiki, Tsukuba, Ibaraki 305-0044

[3]Graduate School of Frontier Science, The University of Tokyo, Kashiwa, Chiba 277-0827

E-mail: SHRESTHA.Lokkumar@nims.go.jp, camsa2@iacs.res.in, ARIGA.Katsuhiko@nims.go.jp

Received: January 31, 2017; Accepted: February 17, 2017; Web Released: February 24, 2017

Lok Kumar Shrestha
Lok Kumar Shrestha received his Ph.D. degree from Yokohama National University (YNU), Japan. He is currently a senior researcher of World Premier International (WPI) Research Centre for Materials Nanoarchitectonics (MANA), the National Institute for Materials Science (NIMS). His current research includes self-assembled fullerene crystals design from zero-to-higher dimensions, mesoporous fullerene crystals and their conversion into graphitic mesoporous carbons, high surface area nanoporous carbon material design from agro-waste for electrochemical supercapacitors and VOC adsorption.

Somobrata Acharya
Somobrata Acharya received his Ph.D. degree from Jadavpur University, India. He is currently Associate Professor in the Centre for Advanced Materials (CAM), Indian Association for the Cultivation of Science (IACS), India. He is carrying out research in interdisciplinary areas probing structure–property relationship and possible applications of semiconductor nanomaterials in the areas of energy generation and consumption. His research area includes heterostructures, 2D nanostructures, superlattices, supramolecular assemblies and their suitable applications.

Katsuhiko Ariga
Katsuhiko Ariga received his Ph.D. degree from Tokyo Institute of Technology. He is currently the Director of Supermolecules Group and Principal Investigator of World Premier International (WPI) Research Centre for Materials Nanoarchitectonics (MANA), the National Institute for Materials Science (NIMS). His research is oriented to supramolecular chemistry, surface science, and functional nanomaterials (Langmuir–Blodgett film, layer-by-layer assembly, self-organized materials, sensing and drug delivery, molecular recognition, mesoporous material, etc. and he is now trying to combine them into a unified field.

Abstract

Designing nanoscale components and units into functional defined systems and materials has recently received attention as a nanoarchitectonics approach. In particular, exploration of nanoarchitectonics in two-dimensions (2D) has made great progress these days. Basically, 2D nanomaterials are a center of interest owing to the large surface areas suitable for a variety of surface active applications. The increasing demands for alternative energy generation have significantly promoted the rational design and fabrication of a variety of 2D nanomaterials since the discovery of graphene. In 2D nanomaterials, the charge carriers are confined along the thickness while being allowed to move along the plane. Owing to the large planar area, 2D nanomaterials are highly sensitive to external stimuli, a characteristic suitable for a variety of surface active applications including electrochemistry. Because of the unique

structures and multifunctionalities, 2D nanomaterials have stimulated great interest in the field of energy conversion and storage. This review highlights recent progress in the synthesis of a variety of 2D nanomaterials and their applications in energy conversion and storage. Finally, opportunities and some critical challenges in these fields are addressed.

1. Introduction

Energy management, including energy generation, conversion and storage is one of the most crucial and greatest challenges in the 21st century.[1–15] Although these targets are in enormous earth-level scales, the most important key for scientific and technical efforts for the target is indeed control of nanoscale materials and structures.[16–24] Not limited to the traditional nanotechnology concept, an emerging concept, nanoarchitectonics, fulfills more and more important tasks.[25–31] This innovative concept was originally proposed by Masakazu Aono to induce a paradigm shift of nanoscale science through establishing methodologies for material architecture fabrication upon arranging nanoscale components. Although nanotechnology tends to handle nanoscale events individually, the nanoarchitectonics approaches are done upon harmonies of mutual interactions and components and finally create hyperfine structures from nanoscale building block components. Recently, the nanoarchitectonics concept has been applied in many research fields such as nano/molecular-scale control,[32–35] fabrication and synthesis of nanostructured materials,[36–40] physical device applications,[41,42] sensors,[43–46] environmental remediation,[47,48] catalysis,[49–51] dynamic processes[52] and biological/biomedical applications.[53–57] It also includes energy fields such as capacitors,[58,59] batteries,[60,61] and energy production.[62] Discovery of useful nanocomponents would promote developments of this nanoarchitectonics approach. Indeed, recent key components are two-dimensional (2D) materials.

The discovery of graphene has generated great interest in 2D materials owing to the immense potential in both basic and applied research.[63,64] Graphene exhibits many unconventional properties, such as large theoretical specific surface area,[65] excellent optical transparency,[66] high Young's modulus,[67] excellent thermal conductivity,[68] ultrahigh carrier mobility at room temperature,[69] integral quantum hall effect (IQHE)[70] and other interesting characteristics like Dirac-cone structure.[71] These interesting properties of graphene have generated tremendous interests in exploring other 2D nanomaterials with versatile properties such as metal dichalcogenides (TMDs; MoS_2, TiS_2, TaS_2, WS_2, $MoSe_2$, WSe_2, etc.),[72–76] hexagonal boron nitride (h-BN),[77] graphitic carbon nitride (g-C_3N_4),[78] compounds of group-IV elements, binary group III–V materials,[79] layered metal oxides, layered double hydroxides and many more (Figure 1).[80,81] Non-layered types of 2D materials such as metals,[82–85] metal organic frameworks,[86,87] covalent organic frameworks,[88] polymers,[89,90] MXenes,[91] black phos-

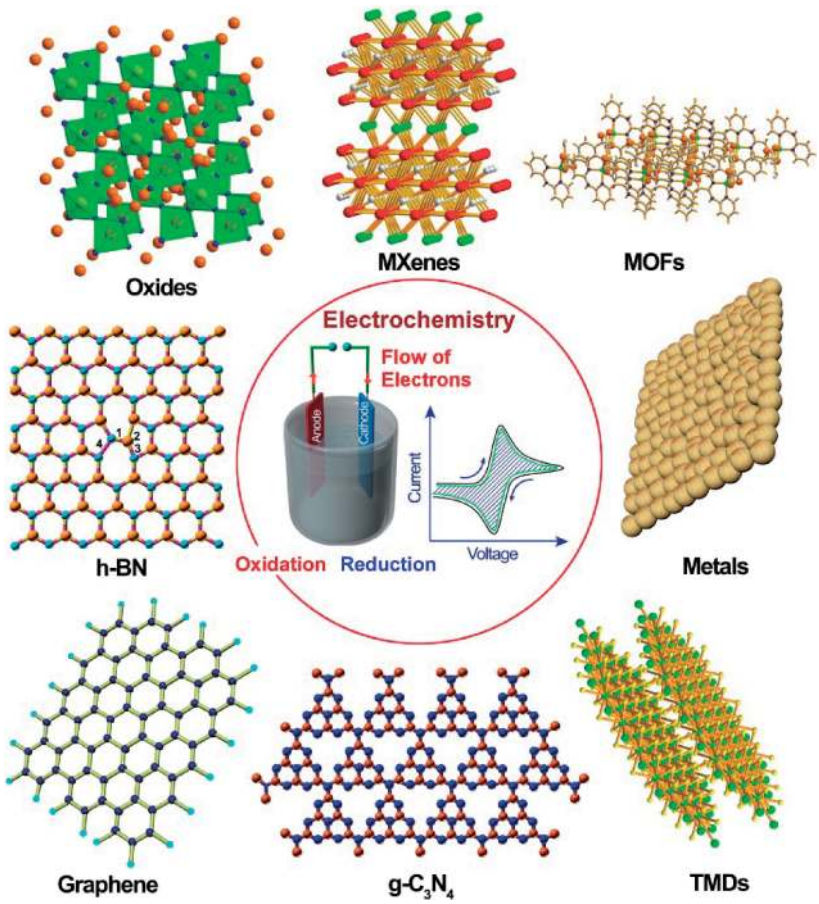

Figure 1. Schematic illustration of different kinds of 2D nanomaterials used in electrochemistry.

phorus,[92] and silicone[93] have also been explored in the recent past (Figure 1).

The 2D nanomaterials possess unique characteristics compared to other shapes of nanomaterials including zero-dimensional (0D) quantum dots (QDs), one-dimensional (1D) nanorods/nanowires, and three-dimensional (3D) networks or even the bulk counterparts. Although the charge carriers are confined along the thickness in 2D nanomaterials, they are allowed to move along the plane. This unique feature renders them appealing candidates for fundamental condensed matter studies and electronic device applications.[63,94] Electronic properties can be precisely tuned by controlling the thickness of 2D nanomaterials, which is not possible in 0D, 1D and 3D nanomaterials. Importantly, the narrow thickness of 2D nanomaterials imposes mechanical flexibility and often optical transparency, which are promising properties for highly flexible and transparent optoelectronic devices. Additionally, the large planar area and narrow thickness generate high specific surface area suitable for surface active applications.[72–81] Owing to the large surface area, 2D nanomaterials are highly sensitive to external stimuli, such as chemical modification, adsorption of other molecules or materials, chemical doping and mechanical deformation.[72–81] These morphological advantages along with the outstanding properties make 2D nanomaterials promising in a wide range of applications including electrochemistry, catalysis, optoelectronics, energy storage and conversion, biomedicine, sensors and many more.

In the field of electrochemistry, 2D nanomaterials are promising candidates to enhance the efficiency of electrochemical sensing, electrochemical energy conversion and storage devices. The large surface area of 2D nanomaterials is highly suitable for electrochemical reactions. Additionally, the 2D nature facilitates the migration of photogenerated carriers thereby reducing the possibility of electron–hole recombination and potentially enhancing the electrochemical performance. In this review, we first describe the preparation methods of various 2D nanomaterials, since the synthesis route has strong influence on the materials properties. The description of fundamental electrochemical properties of the 2D materials with numerous applications in various electrochemical devices starting from energy generation and storage will be described successively.

2. Preparation and Properties

In recent times, enormous efforts have been devoted to explore a variety of reliable methods for the preparation of 2D nanomaterials and to explore the structure–property relationships along with suitable applications. Broadly, 2D nanomaterials have been developed using top-down and bottom-up approaches respectively. In top-down approaches, the van der Waals interaction between the stacked layers of layered bulk crystals is removed to obtain single- or few layer 2D nanomaterials.[95] To date, most ultrathin 2D nanomaterials are obtained from layered bulk crystals. These classes of materials consist of strong intraplane covalent bonding, though, with weak interplane van der Waals interactions. An example includes bulk graphite, which consists of weakly stacked graphene monolayers. The examples of the top-down methods include exfoliation of layered bulk crystals by mechanical cleavage in solid state,[96–102] liquid phase exfoliation in solution phase,[95,103–109] chemical and electrochemical ion-intercalation and exfoliation routes,[110–118] selective etching and exfoliation and laser thinning technique.[119] In bottom-up methods, the 2D nanomaterials are formed by the direct synthesis of precursors via chemical reactions routes. Two typical examples of bottom-up methods include chemical vapor deposition (CVD)[120–124] and wet-chemical synthesis methods.[82,125–131] In this section, we will highlight a few regularly used methods to produce ultrathin 2D nanomaterials using both the top-down and bottom-up approaches.

2.1 Mechanical Exfoliation Route. The mechanical exfoliation method is commonly referred to as the "Scotch-tape method", since a single layer of 2D nanomaterial can be extracted from the layered bulk crystals using simple Scotch tape (Figure 2a).[96–102] This method is effective in obtaining a single to hundreds of layers of the 2D nanomaterial at a time. Novoselov et al. first applied the mechanical exfoliation route to obtain a single-layer of graphene from highly oriented pyrolytic graphite crystal.[69] Many other types of single- or multi-layered 2D nanomaterials have been obtained from their layered bulk crystals using this procedure. Example includes h-BN, 2D TMDs (MoS_2, $NbSe_2$, TiS_2, TaS_2, WS_2, WSe_2, $TaSe_2$, etc.), $Bi_2Sr_2CaCu_2O_X$, metal oxides, BP, MOFs and many more.[96–102] In this method, the fresh surface of a bulk layered crystal is first attached onto a piece of adhesive tape (Figure 2a). In the next step, the tape is peeled off from the surface to obtain the 2D nanomaterials. Repetitive peeling off the layers by means of the attached Scotch tape eventually yields a greater number of 2D nanomaterials. The resultant 2D nanomaterials can be transferred successively onto appropriate target surfaces (like silicon or silicon dioxide wafers) through wet or dry transfer routes. Imaging like atomic force microscopy (AFM), optical microscopy, scanning tunneling microscopy (STM) or structural tools like high-resolution transmission electron microscopy (HR-TEM) have been used to characterize the 2D nanomaterials. Since the method cannot control the number of 2D nanomaterials at a time, mixtures of single and multiple layers are often found along with the thicker flakes. The simplest approach to detect these 2D nanomaterials is to use optical microscopy (Figure 2b) if the resolution permits. Mechanical exfoliation route has also been implied for preparing single and few-layers of other 2D nanomaterials like MoS_2, WSe_2, Bi_2Te_3, TaS_2, and $TaSe_2$, respectively.[97–102]

It is noteworthy to mention that the mechanical exfoliation method is effective if the bulk counterpart crystals are layered compounds. Since no chemical reaction occurs during the exfoliation process, the resultant 2D nanomaterials retain the same crystal structures of their bulk crystal and also remain stable under ambient conditions. The 2D nanosheets obtained using this route were initially used for studying fundamental and intrinsic properties and for the demonstration of electronic devices.[96–102] However, this method has a few limitations; the production yield is quite low which restricts the applications particularly when a large amount of material is required. Additionally, size, shape and thickness of the exfoliated nanosheets are difficult to control. The size of the nanosheets may vary from a few nanometers to a few hundred micrometers. Moreover, a substrate is always necessary to support the nanosheets

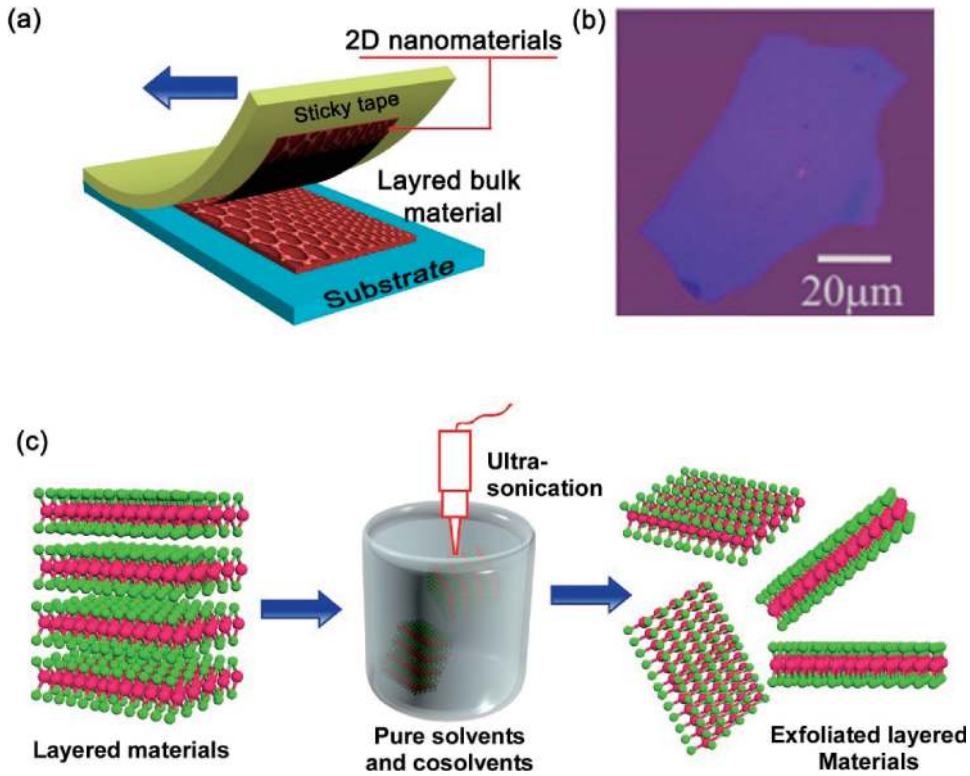

Figure 2. (a) Schematic illustration of the Scotch-tape method to exfoliate 2D nanomaterials mechanically. (b) Digital photograph of large multilayer graphene flake with thickness ~3 nm in normal white light. Ref. 69: *Science* **2004**, *306*, 666. (c) Schematic illustration of the ultrasonication-assisted liquid-phase exfoliation process of 2D nanomaterials.

for realistic applications. Mandatorily, this method requires layered crystals of large dimensions.

The mechanical exfoliation method enables the isolation of single layer graphene with the thinnest dimension retaining the pristine graphene structure.[132] Electronic,[132–134] mechanical,[67] and thermal properties of graphene have been initiated using this route.[68,95] Pristine graphene isolated by mechanical exfoliation is expected to possess poor electrochemical activity.[135] Recently, improved electron transfer kinetics of pristine graphene have been reported based on the corrugations on the graphene sheets.[136] Since the electrochemical applications require a large quantity of material for electrode fabrication, the production yield of the mechanical exfoliation method has to be improved for realistic applications. The presence of a low number of defects on pristine graphene also inhibits the electron transfer properties required for the electrochemical processes. In fact, it was reported that electron transfer events occur about 10^6 times faster at defects or edge-states of carbon materials compared to the defect-free sites.[137] Hence, other fabrication methods to produce 2D nanomaterials have been explored for electrochemical applications.

2.2 Liquid Exfoliation Route. Mechanical exfoliation results in 2D nanomaterials with minimal structural alteration of their layered bulk counterpart. However, this process has been carried out in solid state. Alternatively, liquid exfoliation method can be used to exfoliate layered bulk crystals to obtain 2D nanosheets directly in solvents.[95,103–113] Similar to the mechanical exfoliation route, an external stimulation force (sonication in general) is required in liquid exfoliation to extract the layered structures from their bulk crystals (Figure 2c). Nanosheets of graphene, h-BN, TMDs, metal oxides (like WO_3), metal hydroxides, MOFs, BP have been obtained using liquid exfoliation.[95,103–113] Sonication imparts mechanical forces in the liquid phase, which eventually break the interlayer van der Waals interaction retaining the covalent bonding in the layers. This implies that the efficiency of exfoliation can be increased by comparably matching the surface tension of the solvent with the surface tension of the layer bulk crystal. Solution phase exfoliation of highly ordered pyrolytic graphite (HOPG) was achieved by minimizing the energy loss during exfoliation process using solvents with surface tensions of ~40 mJ m^{-2}.[103] Hernandez et al. obtained graphene sheets in *N*-methylpyrrolidone (NMP) solvent.[103] Blake et al. prepared a graphene suspension by ultrasonication of HOPG in *N*,*N*-dimethylformamide (DMF) solvent.[138] The effect of polarity of organic solvents has also been investigated in detail for the liquid exfoliation method.[139] Eventually, the solvent plays an important role in stabilizing the exfoliated nanosheets by preventing stacking and aggregation. Hence, organic solvents are widely used for efficient exfoliation rather than aqueous solvent, which is prone to induce other physical interactions. However, aqueous solutions containing polymer or surfactant were found to be effective for the liquid exfoliation process. In these cases, polymer or surfactant stabilizes the exfoliated nanosheets when separated from the bulk crystals in aqueous medium.[106] The exfoliation of graphite in aqueous solutions in the presence of sodium dodecyl benzenesulfonate (SDBS), sodium cholate (SC)[140] and 1-pyrenecarboxylic acid were

reported using a sonication approach.[141] However, percussion is required in this method since the use of additional surfactants as exfoliating agents may alter the pristine properties of the resulting nanosheets.[142]

The advantage of liquid exfoliation over the solid exfoliation process lies in simplicity and scaling up the yield of 2D nanomaterials at low cost. Paton et al. explored a high-shear mixing technique of graphite in NMP to obtain graphene nanosheets in large scale.[95] They have observed that the exfoliation process starts above a shear rate of $10^4\,s^{-1}$. They also succeeded in producing other 2D materials like MoS_2, BN, WS_2, $MoSe_2$ and $MoTe_2$ following the liquid exfoliation route using the bulk-layered crystals of corresponding materials. Li et al. obtained a single layer of graphene using disulphuric acid and tetrabutylammonium hydroxide (TBA) intercalated graphite in DMF by the ultra-sonication route.[143] However, the yield of single-layer nanosheets obtained by these methods needs to be improved. Another drawback of sonication is that it relies on breaking the nanosheets into small and inhomogeneous pieces. Valles et al. showed that breaking of nanocrystals may be prevented using preliminary intercalation of graphite with potassium, followed by a spontaneous exfoliation in NMP.[144] Behabtu et al. showed that concentrated single layer graphene can be produced through spontaneous exfoliation of HOPG in chlorosulfonic acid.[145] Hence, the liquid exfoliation method is restricted in terms of the yield and the lateral dimensions of the 2D nanomaterials in terms of the uncontrolled surface area.[145] The solution phase liquid exfoliation method to obtain 2D nanomaterials is certainly an appealing approach. However, the limitations of the quality, dimension and production yield of nanosheets need to be improved. Most of the exfoliated nanosheets remain in a multilayer structure; low reaction yields and lesser control over the dimension of the nanosheets are the major issues to be addressed. The presence of impurities may also affect the electrochemical properties of the 2D nanomaterials. Additionally, the toxic organic solvents and the surfactants used in the exfoliation process are undesirable. Hence, there remains scope for further optimization of the process to achieve high yield product with superior control over the shapes of the 2D nanomaterials.

2.3 Chemical, Electrochemical Ion-Intercalation and Exfoliation. The van der Waals interaction between the adjacent layers of a bulk-layered material can be weakened by the intercalation of ions in the interlayers. Ions like Li^+, F^-, and Ni^{2+} or compounds like sulfuric acid have been used to prepare intercalated graphite by electrochemical methods previously.[146,147] Electrochemical isolation of 2D nanomaterials from layered bulk materials has regained interest after the discovery of graphene.[148] In electrochemical exfoliation, cathodic or anodic potentials are applied in aqueous or organic electrolytes. A bulk layered material (2D nanomaterial to be exfoliated) works as an electrode in the presence of auxiliary (usually Pt) and reference (Standard calomel electrode (SCE) or Ag/AgCl) electrodes (Figure 3a). The layered bulk material is oxidized upon the application of a positive potential causing the intercalation of negatively charged ions from solution into the interlayers of bulk material. In the next step, the application of a negative potential facilitates the exfoliation process by taking out the ions, which supports separation of 2D nanosheets from the bulk material (Figure 3a). Graphene nanosheets from

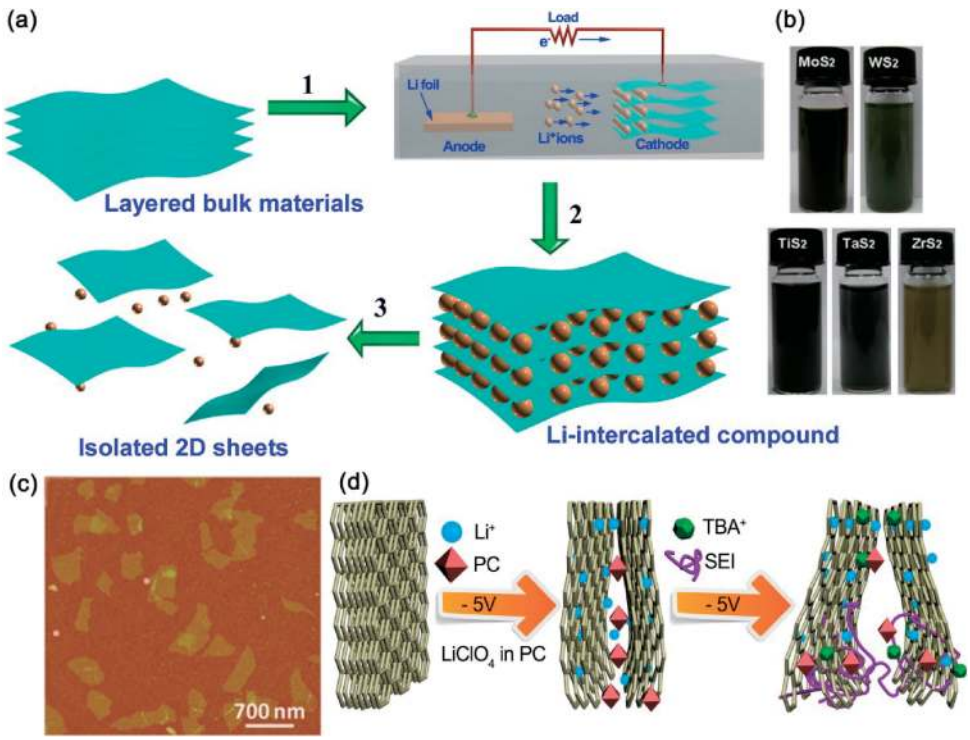

Figure 3. (a) Electrochemical lithiation and exfoliation process for the fabrication of 2D nanomaterials from the layered bulk crystals. (b) Digital photographs of obtained 2D nanosheet dispersions. (c) AFM image of typical large area MoS_2 nanosheets deposited on Si/SiO_2 substrates. Ref. 113: *Angew. Chem. Int. Ed.* **2011**, *50*, 11093. (d) Schematic illustration of electrochemical expansion of graphite. Ref. 154: *J. Am. Chem. Soc.* **2012**, *134*, 17896.

bulk graphite have been fabricated using the electrochemical route in sulfuric acid or poly(styrenesulfonate) medium.[149,150] Sodium dodecyl sulfate molecules have been intercalated into graphitic layers by the application of a positive potential of +2 V followed by reversal of the bias potential to −1 V, which facilitate the exfoliation process. This route yields 2D graphene flakes with an average size of 500 nm in the form of monolayers of graphene.[151]

Ion-intercalation and electrochemical exfoliation methods have been also used to fabricate other 2D nanosheets from their layered bulk crystals. The examples includes h-BN, MoS_2, WS_2, TiS_2, TaS_2, ZrS_2, $NbSe_2$, WSe_2, Sb_2Se_3, and Bi_2Te_3 (Figures 3b and 3c).[113–116] The yields of product using this route are high and yields over 90% for MoS_2 and TaS_2 nanosheets have been reported. Organometallic compounds such as butyllithium and metal naphthalenide (metals = Li, Na, K) were used as intercalators in these cases.[111,112,117] The sonication of intercalated compounds also has resulted in the formation of single- or few-layer nanosheets.[113–118] When layered bulk crystals are immersed in intercalator solution, cations can intercalate into the interlayer spacing of the crystal. Sonication of these ion-intercalated crystals in aqueous phase produces single- or few-layer nanosheets.

Nonoxidized 2D nanosheets can be generated using cathodic reduction/intercalation, retaining the structure. By applying a negative potential, positive ion intercalation process can be achieved. Morales et al. reported on the uses of perchloric acid as an electrolyte, where both the intercalation of H_3O^+ ion at negative potential and perchlorate anion at positive potential were observed.[152] A microwave treatment was performed after the electrochemical process to thermally expand the intercalated layers to obtain 2D nanosheets. Recently, two-stage processes have been reported to improve the yield of the exfoliation process (Figure 3d).[153] In this route, an initial expansion of graphite occurs in a Li^+-containing electrolyte followed by a second expansion step in a tetra-*n*-butylammonium electrolyte. The advantage of this route relies on the application of low potential and ultrasonication treatment is not required to obtain a dispersion of the nanosheets. A direct electrochemical functionalization with aryl diazonium salt with graphite was also demonstrated to obtain functionalized graphene sheets.[153] Li^+ ion intercalation in TMD crystals can induce phase transformation from the semiconducting 2H phase to the metallic 1T phase during the exfoliation process.[111,154] The phase engineering of 2D TMDs offers opportunities for realizing promising applications in electrocatalytic hydrogen evolution, low contact resistance field-emission transistors and high performance electrochemical supercapacitors.[154]

Electrochemical exfoliation methods have several advantages over other exfoliation routes. First, these methods are environmental friendly and the method can be performed under ambient conditions. Secondly, this method offers fabrication and yield of 2D nanomaterials by controlling the applied potential. However, the disadvantage of this method lies in controlling the homogeneous size and layer distribution of the resultant nanosheets. Additionally, this process is highly irreversible. Moreover, the use of anodic potentials to intercalate ions often results in unwanted oxidation while the introduction of oxygen functional groups disrupts the sp^2-hybridized carbon network of graphite. The structural damage and the presence of oxygen functional groups influence the electrochemical properties of the nanosheets. The use of surfactants and polymers in this process may cause irreversible functionalization of the nanosheets which affects electrochemical behaviors.[142] In the case of intercalation by organometallic compounds, the experimental process often requires high temperatures and long reaction times.[111,112] Hence, the preparation process of the electrochemical intercalation method is mild compared to other reported routes.

2.4 Chemical Oxidation, Exfoliation, and Reduction. In this route, chemical species within the interlayer spacing of bulk-layered crystal are intercalated followed by a decomposition process that forces separation of the layers. Oxidative intercalation is a well-established method to separate graphitic layers by means of a strong oxidizing agent. The bulk graphite layered crystal is oxidized by a mixture of potassium permanganate and concentrated sulfuric acid. This process expands the interlayer spacing significantly due to the oxidation and reduces the interlayer strength between adjacent graphene layers. Finally, 2D graphene oxide (GO) nanosheets can be obtained upon applying ultrasonication.[155] However, abundant oxygen containing functional groups remain on the surfaces of GO nanosheets obtained by this route.[156,157] Resultant GO sheets can be reduced to obtain reduced graphene oxide (rGO) sheets by removal of the functional groups from the surfaces.[156] This method is basically a modified Hummers method, which is widely used for the synthesis of graphene sheets.[158,159]

Notably, the reduction of GO sheets has been achieved by using other routes including chemical reduction, thermal annealing, photochemical reduction and electrochemical reduction.[156] Both the GO and rGO sheets are graphene derivatives, however, exhibiting different electronic properties. While graphene is highly conductive, GO is an insulating material. Post synthesis treatments can improve the conductivity of GO, however, to a much lower level than the pristine graphene. The different electronic, chemical and surface properties of GO and rGO sheets make them a different class of nanomaterials with different electronic properties. The presence of functional groups including hydroxyls, epoxides, carbonyls, quinones, and carboxylic acids on their surface allows further chemical functionalization.[76,118,160–165] Because of these oxygen-containing groups, the electrochemistry of rGO not only influences on the heterogeneous electron transfer rate but also on the adsorption/desorption of molecules, which takes place before and after the electrochemical reaction.

2.5 Chemical Vapor Deposition (CVD). The CVD method is widely used to prepare 2D nanomaterials on solid substrates.[82,120–143] In this route, the precursors are allowed to react or decompose at high temperature and high vacuum conditions to grow 2D nanomaterials on solid substrates. This method produces highly crystalline 2D nanomaterials with flexible size and thickness. CVD has been utilized to prepare a wide variety of 2D nanosheets including graphene, TMDs, h-BN, In_2Se_3, Bi_2Se_3 and metal oxides.[120–124] Recently, high-quality large area, single/few layer graphene has been reported by Novoselov et al. using CVD method. CVD grown graphene shows excellent prospects for fabricating transistors, transparent conductive electrodes, electrochemical devices, and corrosion-inhibiting

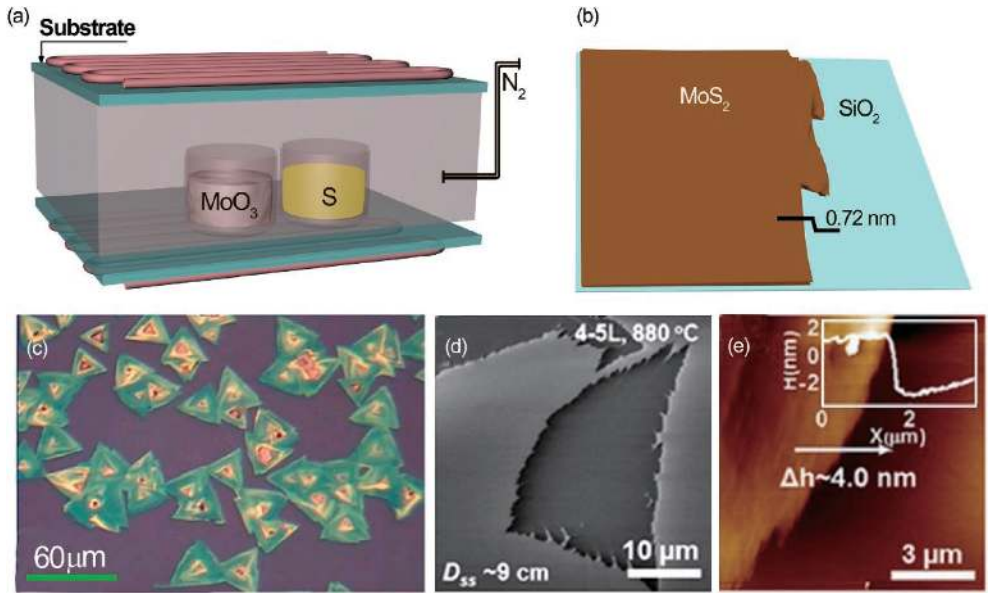

Figure 4. (a) Schematic illustration of an experimental set-up for the CVD-growth of MoS_2 nanosheets. (b) Schematic of a monolayer of the obtained MoS_2 nanosheets on a SiO_2/Si substrate, which was pretreated with rGO demonstrating a thickness of 0.72 nm. (c) Optical micrograph showing the growth of WS_2 layers on the SiO_2/Si substrate pretreated with perylene-3,4,9,10-tetracarboxylic acid tetrapotassium salt (PTAS). Ref. 122: *Adv. Mater.* **2012**, *24*, 2320. (d, e) SEM and AFM images of WS_2 nanosheets grown on sapphire substrates. Inset of panel (e): line profile along the white arrows. Ref. 166: *ACS Nano* **2013**, *7*, 8963.

coatings.[63] However, the electronic and structural properties are still inferior compared to mechanically exfoliated graphene.[165] Synthesis of large area uniform MoS_2 nanosheets on top of SiO_2/Si substrates has been reported by Lee et al. utilizing CVD using MoO_3 and S powders as precursor (Figures 4a and 4b).[122] These authors have observed a similar layer growth behavior of WS_2 on solid substrates, which were treated with graphene-like molecules (Figure 4c). Recently highly crystalline WS_2 nanosheets with domain size exceeding 50×50 μm^2 on sapphire substrate have been reported using chemical vapor deposition (Figures 4d and 4e).[166] Such a large area 2D nanomaterial holds importance for a variety of practical applications based on planar materials. The limitation of CVD lies in the requirement of high temperature, vacuum conditions and requirement of specific solid substrate to support the growth of 2D nanomaterials. Hence, growing 2D materials on flexible substrates at low temperature and vacuum conditions using this technique is a future challenge.

2.6 Wet-Chemical Synthesis. The chemical synthesis route of 2D nanosheets using precursors is one of the best techniques using the bottom-up approach.[82,125–131] This route has been widely used through template synthesis, solvothermal synthesis and colloidal synthesis of 2D nanomaterials. In this route, surfactants are commonly used to control the size, shape and morphology and to impose stability of the as synthesized nanosheets. Numerous 2D nanomaterials such as graphene, h-BN, g-C_3N_4, TMDs, metals, metal oxides, metal chalcogenides, LDHs, MOFs, COFs and polymers have been synthesized using this approach.[82,125–131] Metallic 2D nanosheets such Au, Pd, and Rh; metal oxides including TiO_2, CeO_2, In_2O_3, SnO_2, and Fe_2O_3, as well as metal chalcogenides (PbS, CuS, SnSe, ZnSe, ZnS, and CdSe) were synthesized by route.[82,125–131] Huang et al. reported the hexagonal palladium (Pd) nanosheets by using carbon monoxide as surface coating agent (Figures 5a and 5b).[82] Thickness of these nanosheets lie within 10 atomic layers. These nanosheets exhibit faster electrocatalytic activity for oxidation of formic acid compared to commercially available palladium black catalyst. Gao et al. reported β-$Co(OH)_2$ nanosheets with five-atoms layer thickness by an oriented-attachment technique.[127] Solid-state supercapacitor behavior was obtained allowing an opportunity to realize a supercapacitor at the atomic level. Metal chalcogenide nanosheets of PbS were realized by collective coalescence of PbS nanowires at an air–water interface with the aid of surface pressure using the Langmuir–Blodgett technique (Figure 5c).[129] PbS nanowires were first synthesized using single molecular precursor in trioctylamine surfactants.

A bottom-up synthesis method to generate a series of non-layered metal oxide nanosheets including TiO_2, ZnO, Co_3O_4, WO_3, Fe_3O_4 and MnO_2 in solution phase have been reported by Sun et al. using lamellar reverse micelles (Figures 5d–5f).[128] This transition metal oxide nanosheet contains high surface area and high chemical activity with quantum confinement effect. Solvothermal methods have been used to synthesize zinc chalcogenide nanosheets with a lateral size of ~500 nm with a thickness of ~0.9 nm.[130] Lamellar organic–inorganic intermediates, (Zn_2Se_2)(*n*-propylamine) were first synthesized and the hybrid intermediates were exfoliated by sonication route to obtain freestanding ZnSe nanosheets. The wet-chemical synthesis route allows high reaction yield, easy size and shape control, low cost production of 2D nanosheets. Moreover, the size and shape of 2D nanosheets can be controlled using this route in an easier manner compared to other methods. However, the synthesis route is inherently complicated in terms of understanding the final product. This is because of several reaction parameters such as reaction temperature, reaction time,

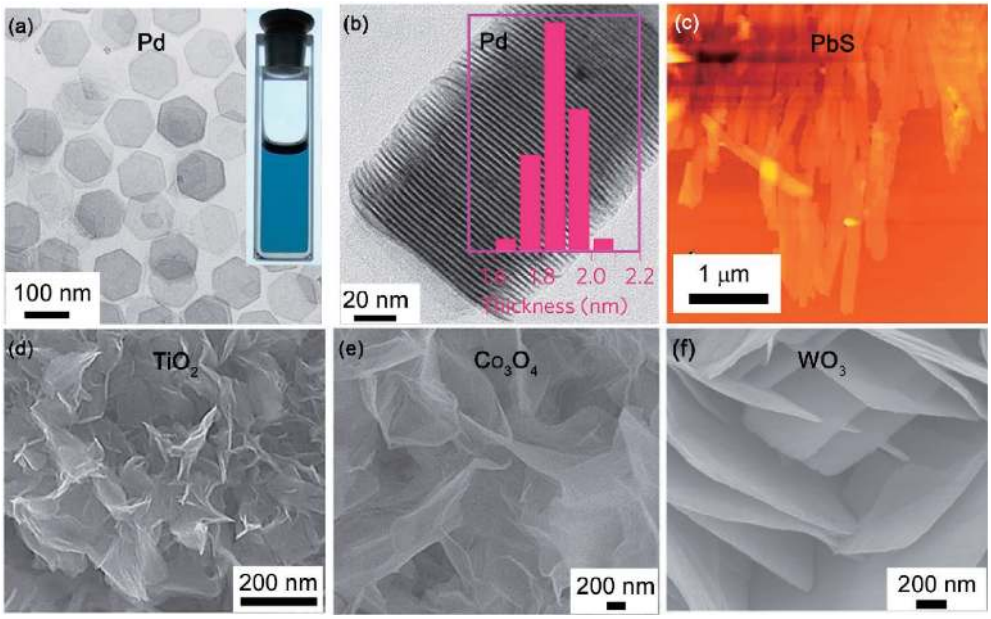

Figure 5. (a) TEM images of Pd nanosheets synthesized in the presence of PVP and CTAB in DMF. Inset: photograph of an ethanol dispersion Pd nanosheets. (b) HR-TEM image of the assembly of Pd nanosheets perpendicular to the TEM grid. Inset: thickness distribution of the Pd nanosheets. Ref. 82: *Nat. Nanotechnol.* **2011**, *6*, 28. (c) AFM topographical image of the PbS nanosheets 3 μm long, arranged in parallel over a large area on mica substrate. Ref. 129: *Nano Lett.* **2013**, *13*, 409. SEM images of ultrathin 2D (d) TiO_2, (e) Co_3O_4 and (f) WO_3 nanosheets. Scale bar, 200 nm. Ref. 128: *Nat. Commun.* **2014**, *5*, 3813.

concentration of precursors, surfactants and solvents, which control the final morphology of the desired product.

3. Application of 2D Nanomaterials in Electrochemistry

2D nanostructures of metals and metal oxides have been widely used as catalysts for clean energy generation and storage applications.[167,168] However, metal-based catalysts are costly to use and they also show low selectivity and durability. Carbonaceous materials are relatively inexpensive metal-free catalysts and are an alternative to the bench mark Pt catalysts.[169] For instance, graphene and its derivatives have been extensively studied as electrode materials due to exceptional physicochemical and electronic properties. Transition-metal dichalcogenides (TMDs) (such as MoX_2 and WX_2) are another class of interesting materials for catalytic applications. In this section, we will overview the recent advancement of 2D nanomaterials for catalysis including electrocatalysis, heterogeneous catalysis and energy storage.

3.1 2D Nanomaterials for Energy Conversion. The performance of an electrochemical device depends on the effectiveness of surface reaction through electronic transfer, transport and kinetic reactions. The electrochemical oxidation of small organic molecules such as methanol, formic acid, glucose etc. has been studied widely for low-temperature fuel cells.[170,171] Direct alcohol fuel cells are attractive for mobile and portable applications such as transportation and electrical power generation.[172] The bench mark catalysts, carbon supported platinum (Pt/C) fuel cells face deficiencies in terms of slow oxygen reduction reaction (ORR) rate, in addition to the higher cost of platinum. Moreover, low catalytic efficiency due to CO poisoning and thermal instability requires resolution for realistic fuel cell application.[173] Highly active catalysts for the ORRs in efficient clean energy conversion in fuel cells and batteries have long been the key to optimize the performance of these devices. In order to maximize the use of metal catalysts, Pt nanomaterials supported with low cost porous materials have been utilized to reduce the expensive Pt material consumption. Graphene and graphene derivative such GO and rGO are important materials as carbon supports for electrocatalysts for enhancing electrochemical performance during fuel oxidation.[161,174] Graphene exhibits a wide potential window of 2.5 V in 0.1 M phosphate buffer neutral solution, which is comparable to the traditional glassy carbon electrode (GCE). In this regards, graphene with 2D planar structure employed as a substrate for growing and anchoring noble metal NCs and alloyed metallic NCs, including Pt,[175–177] Au,[178] Pd,[179] PtPd,[180] and PtRu[181] to realize high performance electrocatalytic devices (Figure 6a). Zhang et al. developed polyelectrolyte poly(diallyldimethylammonium chloride) (PDDA) induced reduction of exfoliated graphite oxide as a facile route to the synthesis of soluble graphene nanosheets.[182]

For example, Figure 6b illustrates a wrinkled thin sheet of graphene and the corresponding SAED shows well-defined six-fold-symmetry in diffraction patterns from the graphene nanosheets (inset of Figure 6b). Highly dispersed Pd nanoparticles have been synthesized on the surface of graphene nanosheets (Figure 6c). The Pd/graphene composite demonstrates excellent catalytic activity for electro-oxidation of formic acid (HCOOH) in comparison to commercially available Pd/XC-72 catalyst. Chronoamperometry curves suggested that Pd/graphene composite is a better catalyst than Pd/XC-72 toward HCOOH oxidation. Additionally, GO and rGO can be used as an alternative carbon support for achieving enhanced

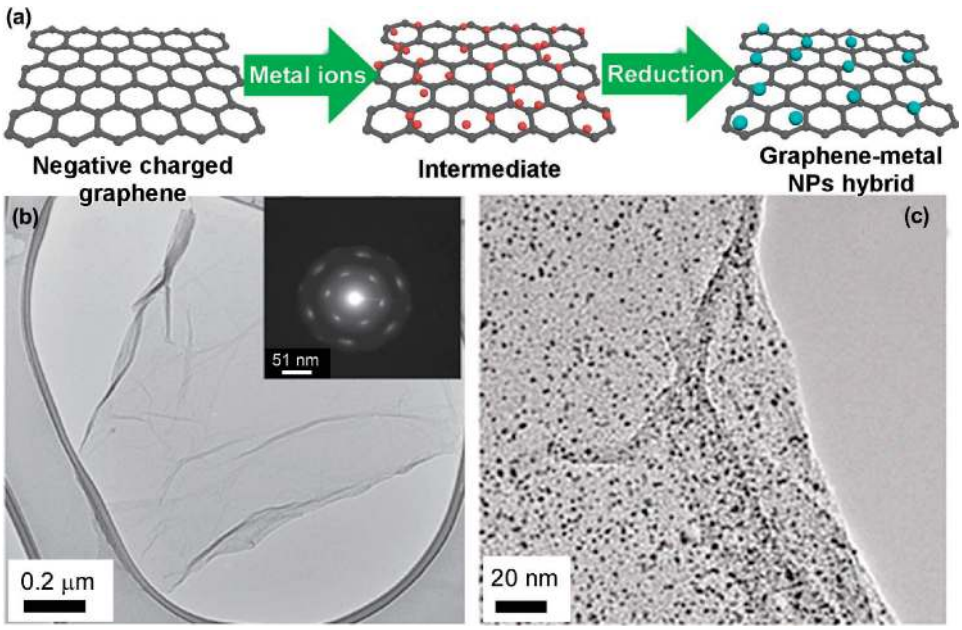

Figure 6. (a) Schematic representation of graphene-metal NCs hybrids. (b) TEM image with SAED pattern in the inset. (c) TEM image of Pd/graphene composite. Ref. 182: *ACS Nano* **2011**, *5*, 1785.

electrochemical performance of catalysts.[161,174] High surface area, superior charge carrier mobility and excellent conductivity of graphene and its derivatives have made them ideal substrates for growing various metal and metal oxide nanocomposites.[67,183–186]

An interesting route to synthesize indium tin oxide (ITO) nanocrystals directly on functionalized graphene sheets was reported by Kou et al.[187] A stable metal–metal oxide–graphene triple junction for electrocatalysis applications has also been reported. For example, Pt-ITO-graphene demonstrated superior catalytic activity for oxygen reduction reaction (ORR) with high mass activity (108 A g^{-1} Pt) and improved stability. The mass activity of Pt-ITO-graphene decreases to 84 A g^{-1} Pt retaining 77.8% activity even after accelerated degradation test protocol. In this case, the defects and functional groups on graphene play an important role in stabilizing the catalysts as suggested by DFT calculations. Ghosh et al. demonstrated graphene nanosheets in combination with Nafion to improve the electrocatalytic activity and durability of Pd catalysts for alcohol fuel cells.[188] In this context, it is worthy of mention that graphene sheets act as 2D substrate to prevent NPs aggregation within the nanocomposites.[176,189–193]

Recently, Ghosh et al. also developed a radiolytic synthesis of mono-metallic and multi-metallic nanoparticles on graphene nanosheets.[194] The graphene supported gold-based multimetallic nanocomposites are used as a highly effective electrocatalyst for glucose fuel cells producing electricity. Similarly, the hybrids with non-precious metal or metal oxides such as iron and cobalt can be used for enhancing the catalytic activity. Moreover, graphene nanosheets can be utilized as metal-free catalysts with superior physicochemical properties and good stability under harsh environments for electrocatalysis of oxygen.[195–197] Further, carbon materials doped with heteroatoms such as boron, nitrogen and phosphorus have become the focus of ORR catalysts due to their high catalytic activity and improved stability. A schematic illustration of ORR is shown in Figure 7a. Recent studies have shown the use of heteroatom (such as N, S and P) doped graphene nanosheets for the efficient ORR applications.[198–200]

Carbon nanostructures and their doping or surface modifications are suitable for tailor made catalytic applications. Dai and co-workers developed edge-rich dopant-free graphene by a one-step and four-electron pathway as efficient ORR electrocatalyst.[201,202] The onset potential of the ORR on an untreated graphene electrode is at 0.76 V (vs. RHE) with the cathodic reduction peak at around 0.59 V (vs. RHE). In contrast, the onset potential and reduction peak of the edge-rich graphene (P–G) shifted positively to around 0.87 and 0.70 V (vs. RHE). The shift of the onset potential and the reduction peak potential of the ORR clearly demonstrated a significant enhancement in the ORR electrocatalytic activity of the edge-rich graphene relative to the pristine graphene electrode. Notably, the size effect of graphene on ORR catalysis was demonstrated by Deng et al.[203] The catalytic activity was found to increase for the smaller size of graphene at different fixed voltages. Jeon et al. developed edge-functionalized graphite (EFG) doped with nitrogen, which exhibited better ORR activity than its counterparts.[204] They have also shown that nanoribbons of boron and nitrogen substituted graphene serve as efficient electrocatalysts for ORR. These Co-doped composites showed the highest onset and half-wave potentials among the reported metal-free catalysts compared to commercially available Pt/C catalyst. The excellent electrocatalytic properties were attributed to the abundant edges of boron and nitrogen Co-doped graphene nanoribbons. It significantly reduces the energy barriers of the ORR reaction as evidenced from first-principles calculations.[205]

Graphitic carbon nitride (g-C_3N_4) is another carbonaceous material with a planar phase analogous to graphite. The g-C_3N_4 possesses interesting properties such as appropriate bandgap, rich density of states at band edge, rich Lewis basic functions,

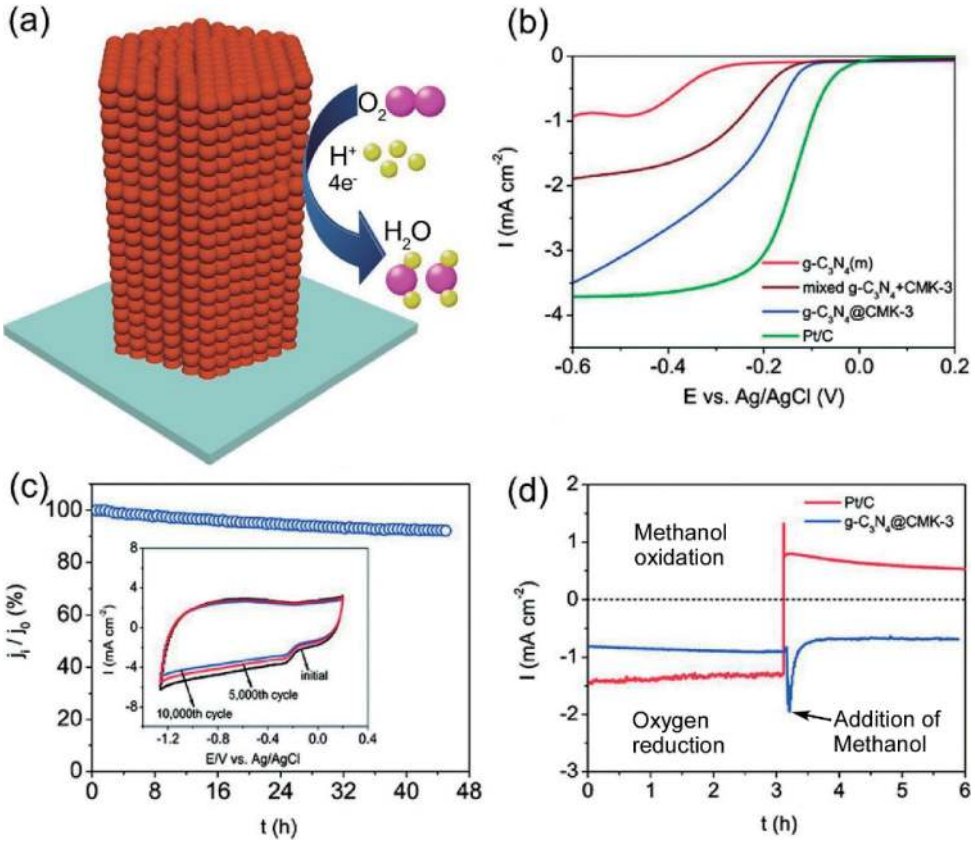

Figure 7. (a) Schematic representation of ORR in presence of electrocatalyst. (b) LSV of various electrocatalysts on RDE at 1500 rpm in O_2-saturated 0.1 M KOH solution. (c) Current–time (*i* versus *t*) chronoamperometric response of g-C_3N_4@CMK-3 at 0.3 V; inset represents cyclic voltammograms under continuous potentiodynamic sweeps. (d) Chronoamperometric responses of Pt/C and g-C_3N_4@CMK-3 at 0.3 V in O_2-saturated 0.1 M KOH solution without methanol and with methanol. Ref. 208: *J. Am. Chem. Soc.* **2011**, *33*, 20116.

Brönsted basic functions and H-bonding motif for the electrocatalysis. Lyth et al. reported ORR catalytic activity of g-C_3N_4 with a higher onset potential of 0.69 V (vs. NHE) compared to 0.45 V for a carbon black reference electrode (XC-72R, Cabot).[206] Yang et al. reported sandwich patterned g-C_3N_4 as metal-free electrocatalysts for ORR.[207] Excellent performance was realized owing to the easy access of oxygen atoms on the catalyst surface and the rapid diffusion of electrons in the electrode. However, the electrocatalysis process showed relatively low current density for the carbon nitride electrode due to poor electric conductivity. To enhance the electron transfer efficiency, Zheng et al. incorporated g-C_3N_4 into mesoporous carbon which exhibits an improved catalytic activity.[208] Mesoporous carbon modified g-C_3N_4 demonstrated a kinetic-limiting current density of 11.3 mA/cm^2 at −0.6 V for a nearly 100% four electron ORR process with superior methanol tolerance (Figure 7b). As prepared catalyst exhibited high stability and a high relative current of 92.2% persisted for prolonged time. Cyclic voltammetry (CV) also reveals reliability with less than 10% cathodic current loss during ~10,000 continuous potential cycles (Figure 7c). Additionally, cathodic ORR current under 0.3 V did not show a significant change after sequential addition of methanol. This indicates that ORR performance was not affected by the addition of methanol which is a frequent problem in the case of benchmark Pt based catalysts (Figure 7d). This exceptional stability was attributed to the homogeneous interactions of the g-C_3N_4 catalyst with CMK-3 support.

Oxygen evolution reaction (OER) and hydrogen evolution reaction (HER) are similar to the ORR for metal–air batteries and electrochemical water-splitting systems. In contrast to Pt-based metal catalysts,[209,210] metal oxides (e.g., iridium, vanadium oxides) are frequently used in fuel cells and lithium–air batteries.[211–214] Alternatively, Zheng et al. demonstrated graphitic-carbon nitride supported by nitrogen-doped graphene (g-C_3N_4@NG) as a metal-free HER catalyst with an unexpected hydrogen evolution reaction activity.[215] Graphitic carbon nitride nanosheet–carbon nanotube 3D porous composites (g-C_3N_4 NS–CNT) display higher catalytic OER activity and stronger durability than Ir-based noble-metal catalysts.[216] The excellent OER activity of g-C_3N_4 NS–CNT originates from high N content of active sites and unique porous architecture that facilitates mass transport and superior electron conductivity due to strong coupling between the g-C_3N_4 NSs and CNTs.

Molybdenum (Mo) based catalysts have been widely explored in HER as they meet the criteria of a low-cost, abundant and non-polluting catalyst.[217] The schematic illustration shows the evolution of H_2 (HER) gas at cathode and evolution of O_2 (OER) gas in anode in presence of suitable electrocatalyst and electrolyte (Figure 8a). Specifically, 2D MoS_2 with a single layer comprising two mono atomic planes of hexagonally

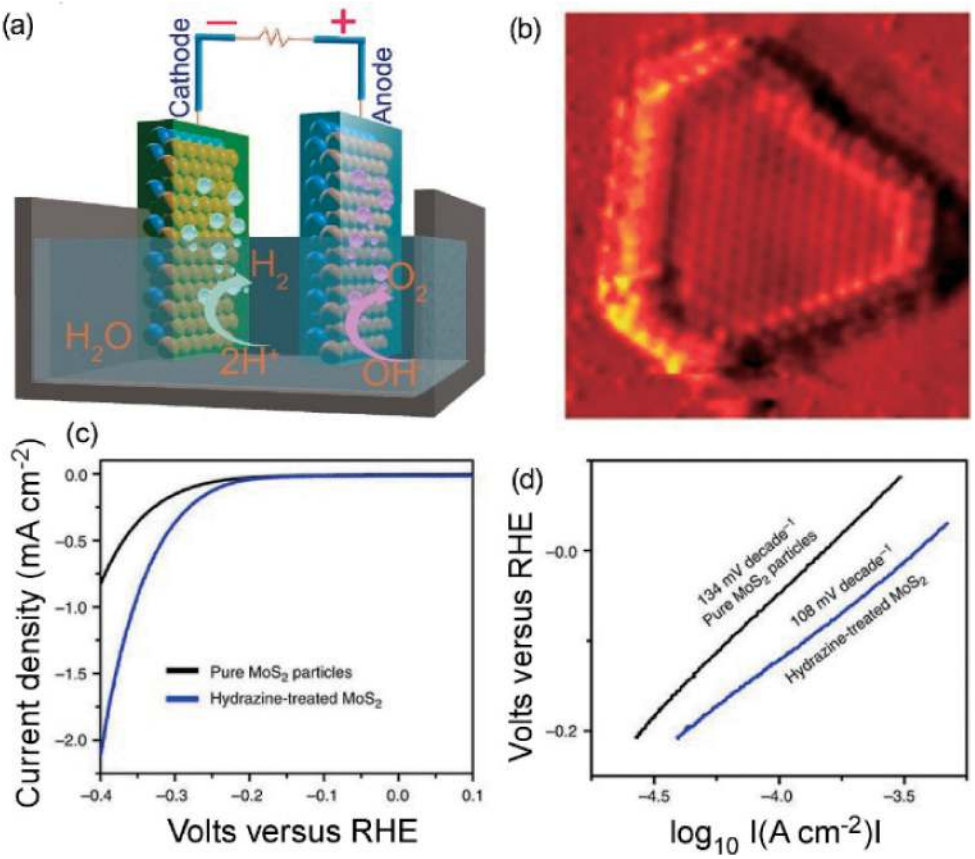

Figure 8. (a) Schematic representation of HER and OER in the presence of electrocatalyst and electrolyte. (b) STM image of atomically resolved MoS_2 nanoparticle on Au(111) showing the predominance of the sulfided Mo-edge. (c) Linear voltammograms and corresponding (d) Tafel slope analysis of MoS_2 particles before (black curve) and after exposure to dilute hydrazine (blue curve). Ref. 220: *Science* **2007**, *317*, 100, Ref. 221: *Nat. Commun.* **2016**, *7*, 11857.

arranged sulphur atoms linked to molybdenum atoms, revealed promising results as HER catalysts.[205,218,219] Interestingly, 2D MoS_2 nanosheets possess enhanced active sites compared to its bulk counterpart. Consequently, defect containing sheets of MoS_2 showed better catalytic activity due to the larger number of exposed edges.[210] Jaramillo et al. reported different sizes of MoS_2 nanomaterials on Au(111).[220] Polygon morphology with conducting edge states on the Au surface was observed (Figure 8b). Electrocatalytic activity for hydrogen evolution correlates linearly with the number of edge sites on the MoS_2 catalyst. The volcano-type relations observed for MoS_2 polygons and the exchange current density as a function of the DFT-calculated free energy of adsorption of hydrogen was determined to be $+0.08$ eV for the MoS_2 edge. MoS_2 structures possess high surface area and a conductive reduced oxide core, which are useful for high catalytic activity. However, an inert basal plane reducing the available active edge sites during the synthesis of MoS_2 imposes a barrier to this system. This results in lowering the catalytic activity for HER beneath the theoretically achievable limit. Chemical modification of the MoS_2 inert basal planes helped increasing the charge carrier concentration for the further improvement in electrocatalytic activity.

Cummins and co-workers exposed MoS_2 2D sheets to dilute hydrazine (N_2H_4) to improve catalytic activity towards HER.[221] A significant improvement in catalytic activity with a 10-fold increase in current density ($\sim$2 to 22 mA cm^{-2}) was observed. This result demonstrates one of the lowest reported HER overpotentials ($\sim$100 mV versus the reversible hydrogen electrode, RHE) for any MoS_2 architecture. The MoS_2 powder consists of several tens of molecular MoS_2 layers in random orientations. The linear voltammetry plot shows poor catalytic activity for the HER. However, the hydrazine treatment improves both the current density and HER activity (Figure 8c). Tafel analysis shows a decrease in the Tafel slope of the pure 2H-MoS_2 particles indicating an increase in proton absorption onto the catalysis surface (Figure 8d). A decrease in the charge transfer resistance showed improved conductivity after the hydrazine treatment. Hydrazine acts as an electron dopant in MoS_2 increasing its conductivity, which leads to improved electrocatalytic performance. Voiry et al. reported monolayers of chemically exfoliated WS_2 sheets as efficient catalysts for hydrogen evolution with very low overpotentials which are consistent with MoS_2 edges.[222] The bulk powder of WS_2 exhibits poor catalytic activity. The enhanced electrocatalytic activity of WS_2 is associated with the high concentration of the strained metallic 1T (octahedral) phase in the exfoliated WS_2 nanosheets.

The effects of transition metal doping in metal dichalcogenide electronic structures have been carried out to enhance the intrinsic catalytic activity of MoS_2 by altering the free energy of hydrogen adsorption (ΔGH) on the edges. Chua et al. studied the effects of doping using powder Mo, W, Nb, Ta, and

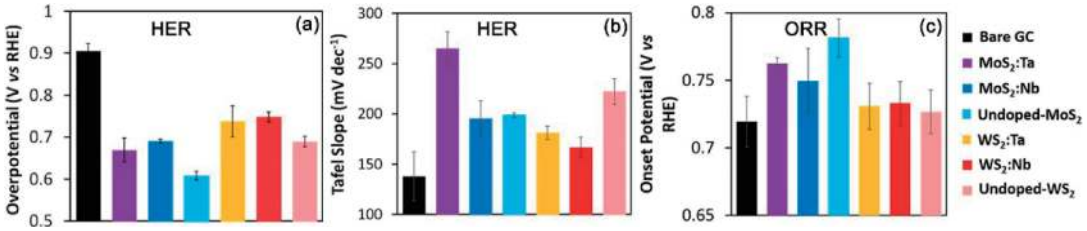

Figure 9. Consolidated data for HER analysis. (a) Bar chart for a comparison of the HER overpotential of bare GC, Ta-doped MoS_2, Nb-doped MoS_2, undoped MoS_2, Ta-doped WS_2, Nb-doped WS_2, and undoped WS_2 (b) Bar chart comparing the Tafel slope. (c) The onset potential of the ORR using the potential at which 10% of the maximum current is achieved. Error bars correspond to the standard deviations on the basis of triplicate measurements. Ref. 223: *ACS Catal.* **2016**, *6*, 5724.

Table 1. Summary of 2D materials for applications in catalysis

2D material	Catalytic system	Performance or parameter	Ref.
2D metal crystals (for example Pd)	Electrocatalytic oxidation of formic acid	Activity is 2.5 times that of Pd black catalyst	82
Graphene with defects	Oxygen reduction reaction (ORR) in alkaline conditions	Carbon atoms at edges or defects act as additional active sites	201, 203
Graphene doped with other heteroatoms (such as N, B, S, P, O or metal)	ORR in alkaline conditions	Catalytic activity is comparable to Pt/C Heteroatoms can affect the charge distribution and electronic states of carbon atoms and hence both hetero-and carbon atoms act as active sites	204, 205
Graphitic C_3N_4 ($g\text{-}C_3N_4$)	ORR in alkaline conditions Electrocatalytic water-splitting	A kinetic current of 7.3 mA cm^{-2}, superior to that of commercial Pt/C Activity of both the hydrogen and oxygen evolution can be enhanced	206–208, 215, 216
2D pure transition metal dichalcogenides (such as MoS_2, WS_2) and with heteroatoms	Electrocatalytic HER in acidic medium	Edges of pure MoS_2 are considered to be the active sites. Dopant heteroatoms can enhance the activity of the surface S atoms	220, 237
Heterostructures based on 2D nanocrystals	Electrocatalytic HER	Enhance the HER activity Charge transfer between different layers can modify electronic properties and reactivity	225, 236, 238, 239

S on MoS_2 and WS_2 layered TMDs for both HER and ORR with p-dopants Nb and Ta.[223] The doping in MoS_2 and WS_2 showed significant effects in the catalytic activity for the HER and ORR (Figure 9). The lowest observed overpotential (the potential at which the redox process is experimentally observed) is 0.61 V (versus RHE) for undoped MoS_2 (Figure 9a). The doped TMDs (MoS_2 and WS_2) are catalytically more effective compared to their undoped counterparts for the HER. A comparison of the overpotential at a current density of $-10\,mA\,cm^{-2}$ is shown in Figure 9a. This suggests that the overpotential at $-10\,mA\,cm^{-2}$ is the lowest for the MoS_2 compounds, followed by the WS_2 group. It has been found that the doped materials have a higher overpotential than their respective undoped TMDs for HER. Tafel analysis reveals that Nb-doped TMDs have a lower Tafel slope in comparison to Ta-doped TMDs. The doped WS_2 results in a decrease in Tafel slope (Figure 9b). This trend was not observed for MoS_2. On the other hand, doped MoS_2 and doped WS_2 both were able to catalyze the ORR (Figure 9c). Doped TMDs are more catalytic in comparison to bare glassy carbon (GC) showing a more positive onset potential.

Enhanced performances have also been observed on MoS_2/graphene,[224,225] MoO_3/MoS_2[226] and MoS_2/Au[227] composite catalysts for H_2 production. Efforts have been made to explore efficient electrocatalysts by using earth-abundant 3d metal (Co, Ni etc.) chalcogenides.[228–234] Kong et al. also observed HER activities from various polycrystalline transition metal dichalcogenide (MX_2, M = Fe, Co, Ni; X = S, Se) films, especially from the $CoSe_2$.[235] Similarly, Gao et al. developed a highly active and stable HER electrocatalyst in acidic electrolyte based on quasi-amorphous MoS_2-coated $CoSe_2$ hybrid with an onset potential close to commercially available Pt catalyst (Johnson–Matthey, 20 wt% Pt/XC-72).[236] A small Tafel slope of ~36 mV per decade with no current loss after long-term chronoamperometry measurements reveal robust performance amongst the noble-metal-free HER electrocatalysts.[236] Electrocatalytic applications (oxidation of acids, ORR, OER and HER) of various 2D nanomaterials including pure metals, graphene with defects, heteroatom-doped graphene, graphitic carbon nitrides, pure transition-metal dichalcogenides and heterostructures based on 2D nanocrystals are summarized in Table 1.[137–239]

3.2 Energy Storage. The development of novel functional materials for energy storage is of great importance to fulfill the increasing demand for energy. Lithium-ion batteries (LIBs) are promising electrochemical devices for powering porta-

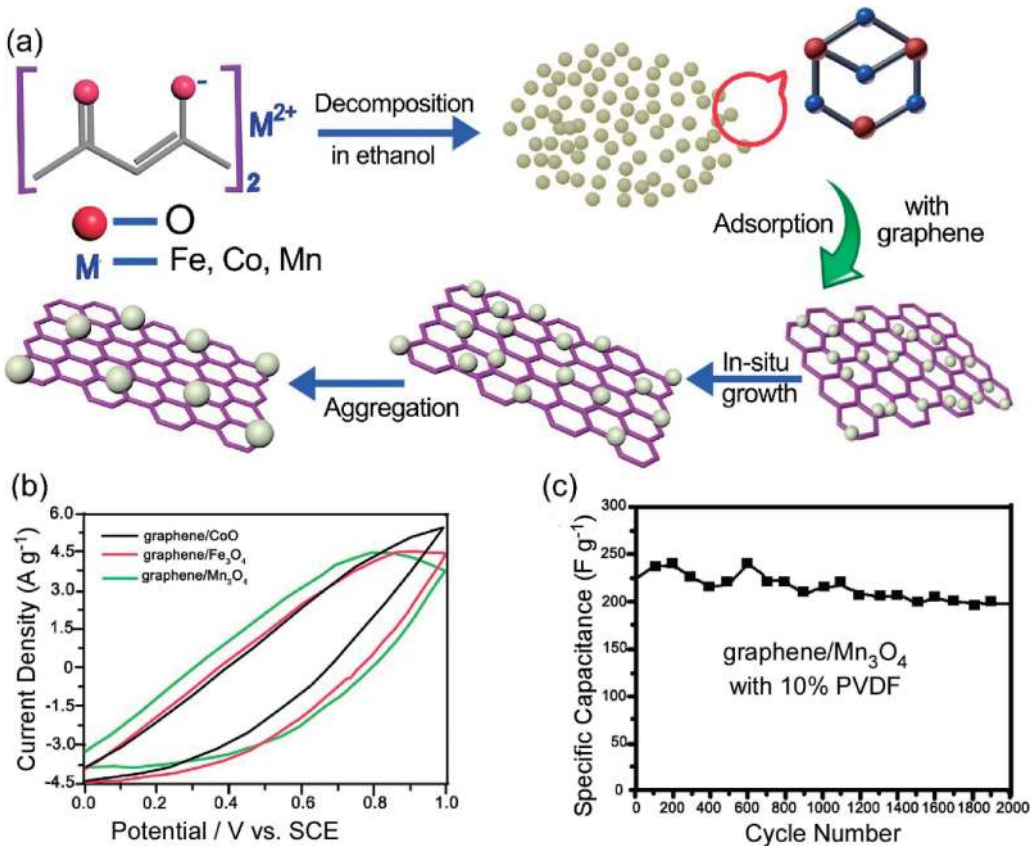

Figure 10. (a) Schematic illustration showing decomposition of metal acetylacetonate to metal oxide nanoparticles followed by the adsorption on graphene and aggregation. (b) CV curves of graphene/Fe_3O_4, graphene/Mn_3O_4 and graphene/CoO composites (c) Long-term cycling performance of a graphene/Mn_3O_4 composite with 10 wt% PVDF. Ref. 262: *Green Chem.* **2012**, *14*, 371.

ble electronic devices, laptops and electric vehicles.[240] On the other hand, supercapacitors are key devices of energy storage due to their high specific capacitance, high power density, ultrafast charging–discharging rate, superior cycle lifetime and extremely low internal discharge.[241,242] 2D nanomaterials including graphene, graphene-like materials, such MXenes and transition-metal dichalcogenide (TMDs) have been explored to develop supercapacitors with enhanced electrochemical performance.[243–246] Graphene-based electrochemical supercapacitors have shown high energy, powder densities and higher Li-storage capacity. These results are associated with the higher ultrathin specific surface area and excellent electronic conductivity to accommodate large number Li^+ ions during the Li^+ ion intercalation process.[247–249] Graphene sheets are extremely attractive for energy storage applications because of their very high theoretical surface area of 2630 $m^2\,g^{-1}$.[250] These extraordinary features of graphene serve as key components in high-performance electrochemical energy storage and conversion devices.

Graphene-based ultracapacitors were developed by Ruoff and co-workers.[65] Yang et al. showed capillary compression of gel-based prototype electrochemical capacitors containing both a volatile and nonvolatile electrolyte with a high packing density.[251] Notably, El-Kady et al. used direct laser induced reduction of graphite oxide films with high electrical conductivity and specific surface area as electrochemical electrodes without using any binders or current collectors.[252] These graphite oxide films exhibit ultrahigh energy density values and excellent cycle stability. However, these 2D nanomaterials showed tendency of aggregation during the electrode fabrication process, which significantly decreases catalytic cycling stability. It is important to study the various experimental aspects such as electrode polarizability, electrolyte dynamics, possible chemical processes, structural defects in the electrodes and pore characteristics of GO and rGO as electrode material in LIB. Hybridization of the 2D nanomaterial with another type of nanomaterial as an effective approach to address these issues. 2D porous graphene hybrids with carbon or metal oxides are excellent examples of anode materials for lithium storage.[253,254]

Additionally, transition-metal oxide nanocrystals such as MnO_x, RuO_2, and Fe_3O_4 have been widely investigated as electrode materials in pseudocapacitors.[255] However, the energy storage capacity for large scale applications is limited owing to their high electrical resistance and poor electrochemical reversibility.[255] Graphene can act as a substrate for better distribution of transition metal oxide NCs for rapid electron transmission. Dispersed metal oxide NCs on the graphene can effectively prevent the stacking of graphene sheets, leading to higher available surface areas for the charge storage (Figure 10a). The electrochemical performance of graphene/Mn_3O_4, graphene/Fe_3O_4 and graphene/CoO composites as supercapacitor anode materials have been investigated.[256] These hybrids were found to exhibit enhanced capacitance compared to that of pristine graphene and pure NCs, and showed high current density while

maintaining long term cycling stability.[257–261] Qian et al. developed a simple, environmentally friendly, chemical approach for decorating the reduced GO with transition-metal (Fe, Mn, Co) oxide NCs.[262] The capacitance of these composites is found to be higher than that of pure rGO and metal oxides NCs. The specific capacitance of as-prepared graphene/Mn_3O_4 composite reaches a value of 239.6 F/g, when employed as the anode material in neutral NaCl electrolyte solutions. These results indicate synergetic effects from both graphene and Mn_3O_4 NCs (Figure 10b).

Moreover, graphene can provide a direct conductive path for oxides metal nanoparticles, without the need of conductive carbon black as fillers. Galvanostatic charge–discharge curves of graphene/Mn_3O_4 composite have been measured at different current densities of 1, 5 and 20 mA cm^{-2}. Figure 10c shows the cycling stability test for graphene/Mn_3O_4 composites. The decrease in capacitance by ~12.6% after 2000 cycles suggests potential for supercapacitor applications. Hence, using high quality exfoliated graphene as a conductive substrate provides efficient electron transfer channels attached to NCs, as well as contributes to double layer capacitance to the overall energy storage. In addition to graphene, metal chalcogenides (e.g., MoS_2, WS_2), MXenes (e.g., Ti_4C_3) and metal hydroxides (e.g., β-$Co(OH)_2$) have also shown promising results as electrodes in supercapacitor devices.[263–267]

MoS_2 is of interest owing to the analogous layered structure of S–Mo–S with graphite as well as its higher intrinsic ionic conductivity with high lithium storage capacity. Ajayan et al. utilized a direct laser-patterned MoS_2 based microsupercapacitor with a volumetric capacitance of 178 F/cm^3 and excellent cyclic performance.[268] Yang and co-workers have synthesized edge-oriented MoS_2 nanoporous films by electrochemical anodization and showed a specific capacity 14.5 mF/cm^2 from galvanostatic charge–discharge measurements.[269] A series of hydrothermally synthesized mesoporous MoS_2 nanostructure have also been reported for high performance supercapacitor applications.[270,271] Chhowalla et al. used metallic 1T-phase MoS_2 nanosheets as promising electrode materials for supercapacitor applications.[272] Nanosheets of MoS_2 were prepared by chemical exfoliation having a metallic 1T phase with high concentration. The prepared materials can electrochemically intercalate several ions such as H^+, Li^+, Na^+ and K^+ with extraordinary efficiency and realize capacitance values ranging from ~400 to ~700 F/cm^3 in a variety of aqueous electrolytes.

Despite the high performance, the structural deterioration of MoS_2 due to a large volume change during charge–discharge cycling limits their large scale application. Attempts have been made to improve the electrical conductivity and the structural stability of MoS_2-based electrode materials. Various carbonaceous materials, such as carbon fibers, carbon spheres, or graphene have been employed to form a composite with MoS_2 for this purpose.[273–275] A carbon component can enhance the conductivity and concurrently buffer the volume changes of MoS_2 during the lithiation–delithiation reaction leading to fast electrode kinetics and stable cycling performance. Chang et al. developed a solution-phase method to prepare a 3D MoS_2/graphene composite that exhibited a specific capacity of ~1100 mAh g^{-1}.[276] A two-step strategy was also proposed by Wang et al. to grow honeycomb-like MoS_2 nanosheets anchored into 3D graphene foam, which displayed a discharge capacity of 1050 mAh g^{-1} at a current density of 200 mA g^{-1} after 60 cycles.[277] Liu et al. developed MoS_2/graphene nanocomposite by hydrolyzing the lithiated MoS_2, which deliver a reversible capacity of 1300–1400 mAh g^{-1}.[278] Teng et al. designed composite nanostructure with MoS_2 nanosheets grown perpendicularly on graphene sheets (MoS_2/G composite) by a facile and scalable hydrothermal method (Figure 11a).[279] The formation of this type of architecture prevents the restacking of graphene sheets as well as agglomeration of MoS_2 nanosheets during charge/discharge processes. MoS_2/G composite employed as an anode of LIB, and electrochemical measurements demonstrates a high reversible capacity, a superior rate capability and a long cycle life. The electrode displays an excellent reversible capacity after 150 cycles retaining 92.8% of the initial reversible capacity and a stable cycle life after 400 cycles (Figures 11b–11c).

The improved performance is associated with a large number of electrochemically active sites due to the vertical growth of MoS_2 nanosheets on the graphene sheets. The MoS_2 NCs ensures facile penetration of the electrolyte and shortens the diffusion path of lithium ions. Hence, graphene-based hierarchical composite can be considered as a promising anode material for high performance LIB. Tang et al. developed a controllable synthesis of sandwiched nanocomposites using PPy ultrathin films on 2D MoS_2 monolayers and consequently used as supercapacitor electrodes with a record high specific capacitance, remarkable rate capability, superior power density and energy density.[280] In another interesting example, Rao and co-workers fabricated conducting polymer-based high performance supercapacitors using polyaniline (PANI) with nanosheets of nitrogen-doped RGO, $BC_{1.5}N$, MoS_2 and WS_2.[281] Notably, 2D nanosheet surfaces control the growth of conducting polymers via strong coordination with nitrogen atoms of PANI or polypyrrole (PPy) with the transition-metal centers of metal dichalcogenides. On the other hand, due to combination metal dichalcogenides with conducting polymers, the poor conductivity of pure MoS_2 can be improved. These systems are ideal for supercapacitor applications with exceptional energy and power density.

Gogotsi and co-workers pioneered as a new family of promising 2D supercapacitor electrode materials, so-called MXenes.[91,267] The MXenes materials are prepared from layered hexagonal MAX phases, which include more than 60 forms of ternary nitrides or carbides. In MAX, M represents an early transition metal (e.g., Ti, V, Cr, Nb, etc.), A denotes an A-group element (e.g., Al, Si, Sn, In, etc.), and X means C or N. They have shown a binder-free $Ti_3C_2T_x$ MXene material with high flexibility and high volumetric capacitance in aqueous electrolyte NaOH.[266] In particular, flexible supercapacitor devices with high performance and long-term stability show great potential for applications in portable electronic devices.[282–285] MXenes considered as flexible and conductive material typically show higher energy storage ability for pseudo-supercapacitor application, compared to carbon-based materials and larger conductivity compared to transition-metal oxides. Gogotsi and co-workers produced multifunctional composite films based on $Ti_3C_2T_x$ MXene with either a charged polydiallyldimethyl-

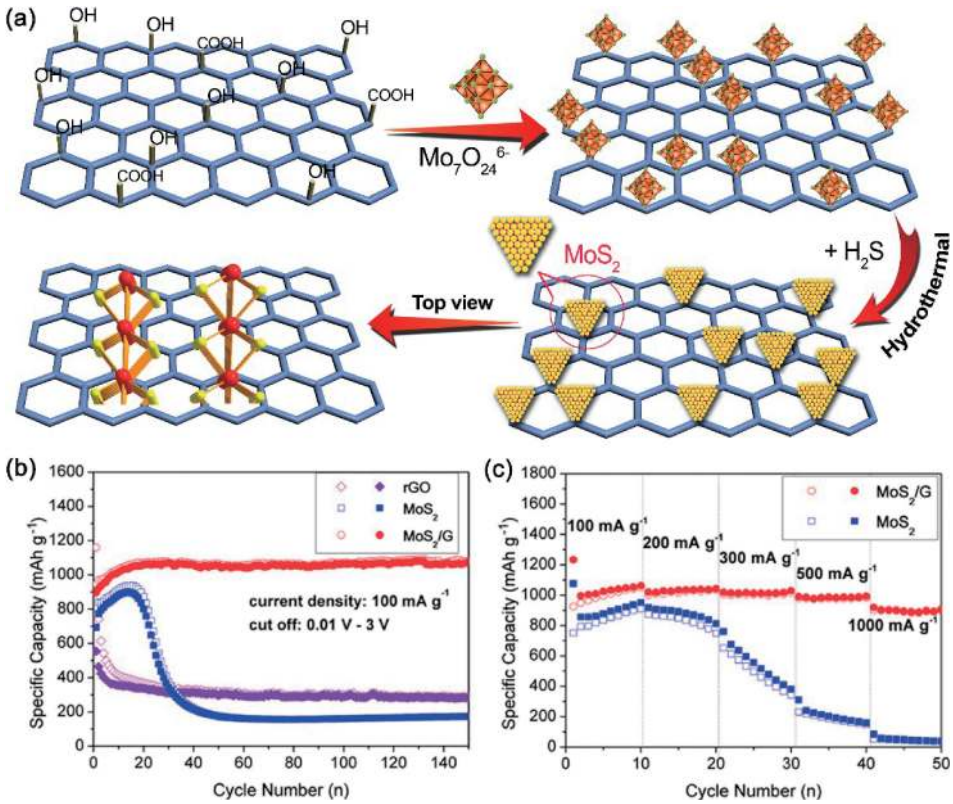

Figure 11. (a) Schematic illustration of the synthesis procedure of MoS_2/G. (b) Cycling performance of MoS_2/G, MoS_2, and rGO electrodes at a current density of 100 mA g^{-1} for 150 cycles. (c) Rate capability of MoS_2 and MoS_2/G. Ref. 279: *ACS Nano* **2016**, *10*, 8526.

ammonium chloride (PDDA) or an electrically neutral polyvinyl alcohol (PVA) with excellent mechanical and electrochemical properties (Figures 12a–12c).[286] These composite films illustrate impressive capacitive performance as high as 528 F/cm^3 for energy storage devices (Figure 12d). To date, the investigation of MXenes-based electrode materials is limited and intensive efforts required along this direction to realize realistic applications.

In contrast to the LIBs, Na-ion batteries (NIBs) can satisfy the requirements of grid-level storage. Na is an earth abundant element and ubiquitous around the globe. In addition, NIBs similarly have a rocking chair operation mechanism with LIBs, which potentially provides high reversibility and long cycling life.[287–290] For example, Yu et al. prepared an interesting structure of embedding single-layered MoS_2 nanoplates in carbon nanofibers, which delivers a high reversible Na ion storage capacity of 854 mA h g^{-1}.[291] A general schematic illustration for various nanocomposite formation is shown in Figure 13. 3D MoS_2–graphene microspheres show a capacity of 322 mA h g^{-1} at a current density of 1.5 A g^{-1}.[292] Sheet-on-sheet structured MoS_2/rGO nanocomposites show a reversible Na ion storage capacity of 338 mA h g^{-1} [293] and 702 mA h g^{-1}, respectively.[294] The high abundance and low cost of Na and its low redox potential (0.3 V above that of lithium) makes rechargeable sodium ion batteries (SIBs) an alternative to LIBs. However, improvement of supercapacitor performance using novel electrode materials accompanied by low-cost production necessitates a deep fundamental understanding of the charge storage mechanisms, transport pathways of electrons and ions and electrochemically active sites.

4. Conclusion

2D materials-based electrochemistry is an extremely important field for energy conversion and storage applications. We reviewed the electrochemical properties of advanced, low cost, recently reported 2D materials for energy applications and storage. 2D nanostructures possess excellent mobility, high surface area, morphology tunability and offers the possibility to tailor the surface properties for various applications in exceptional ways. Hybrid 2D structures have shown high efficiency in terms of energy density although further improvement in fabrication techniques is important in order to contribute widespread implementation of fuel cells and devices. Moreover, it is important to develop low-cost, lightweight and high performance 2D materials, which are prepared by scalable solution processing with earth-abundant and environment-friendly sources to create future energy conversion and storage devices with superior power density and energy density. We believe that understanding the catalytic nature of these 2D materials using in situ characterization techniques, theoretical simulations and combining these with the development of suitable synthetic technology, would create real catalytic-based device applications. For example, Nakamura et al. very recently reported detailed characterization of ORR active sites by using HOPG-based model catalysts with well-controlled nitrogen atom doping.[295] Carbon atoms with Lewis basicity next

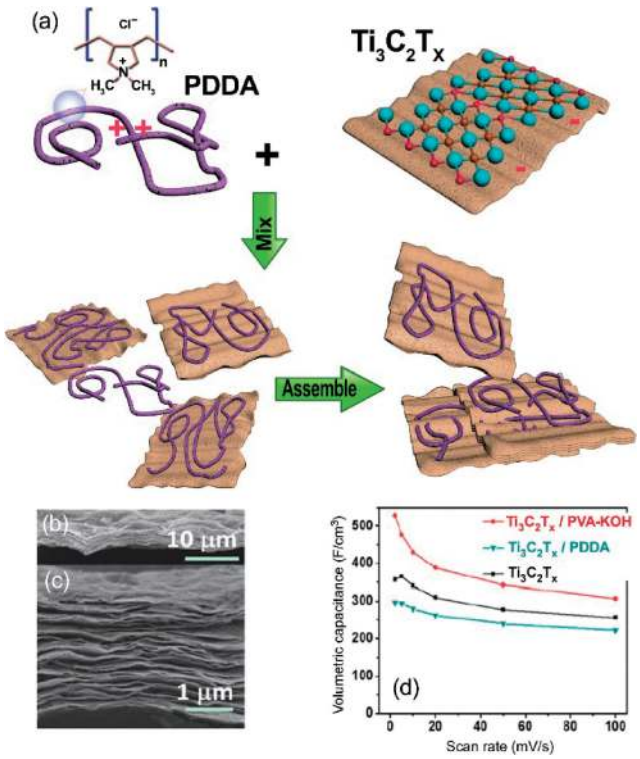

Figure 12. (a) Schematic illustration of synthesis of $Ti_3C_2T_x$/PDDA hybrids and their assembled films. (b and c) Cross-sectional SEM images of the films at different magnifications. (d) Capacitive performance of $Ti_3C_2T_x$, $Ti_3C_2T_x$/PDDA, and $Ti_3C_2T_x$/PVA-KOH films at different scan rates. All electrochemical tests were conducted in 1 M KOH electrolyte, using three-electrode Swagelok cells with over capacitive activated carbon and Ag/AgCl as counter and reference electrodes, respectively. Ref. 286: *Proc. Natl. Acad. Sci. USA* **2014**, *111*, 16676.

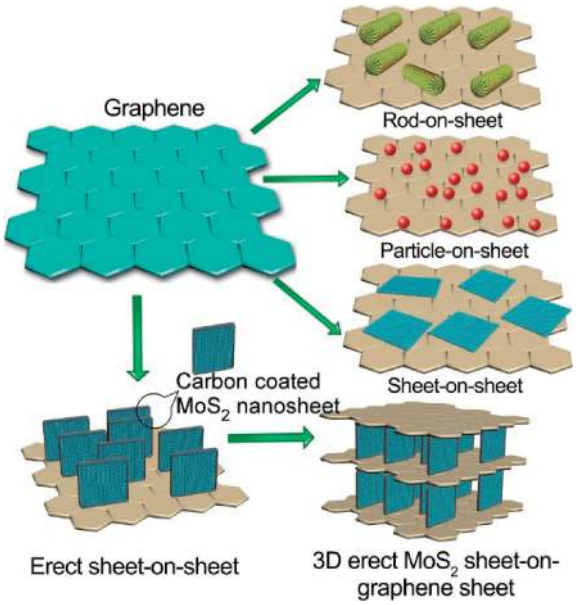

Figure 13. Schematic illustration showing the various graphene-based composite supported MoS_2 of various morphologies. The structure of standing carbon-coated MoS_2 (MoS_2@C) nanosheets on graphene is the main product of this study, which forms a sandwiched 3D porous network after stacking. Ref. 294: *Adv. Funct. Mater.* **2015**, *25*, 1393.

to pyridinic nitrogen atom was revealed as active site for high ORR activity. Such knowledge would be important for designing 2D materials with the best performance. Because 2D nanomaterials can also be good building blocks for developing further complicated structures for advanced functions, 2D nanomaterials will significantly promote developments of electrochemical nanoarchitectonics in energy-related science and technology. Apart from the scientific issues, there are many technological problems such as mass production of 2D materials and their hybrids that need to be addressed for large scale applications.

Further exploration of this research area will create many possibilities. Applicable materials are not limited to 2D materials described above. For example, stable layered black phosphorus and its applications in energy storage, e.g., battery have received much attention.[296–299] These materials can be prepared through various strategies including conventional mechanical exfoliation and vapor transport growth. They have puckered honeycomb lattice and unique properties concerning carrier mobility, a relative low contact resistance, and a wide-range of direct bandgaps. Various applications such as energy storage and conversion, electrochemical catalysis, and sensors have been very recently demonstrated. Conjugation with the other nanostructured materials such as nanoporous materials may create another possibility because their application to wide range of usages have been well investigated.[300–302] For example, direct formation of alternate layer-by-layer structures between graphene oxides (2D materials) and coordination polymers (nanoporous materials) have been reported together with their outstanding electrocatalytic activity and excellent durability for the oxygen reduction reaction.[303] These fabrication processes may be linked even with organic synthetic approaches[304,305] and supramolecular organization.[306,307] However, more important efforts for practical usage and industrial applications would be those for mass production,[63,308–310] which would be a crucial step for further development of 2D materials.

This study was partially supported by JSPS KAKENHI Grant Number JP16H06518 (Coordination Asymmetry) and CREST, JST.

References

1 N. S. Lewis, *Science* **2016**, *351*, aad1920.
2 Z. Xiao, H. Lei, X. Zhang, Y. Zhou, H. Hosono, T. Kamiya, *Bull. Chem. Soc. Jpn.* **2015**, *88*, 1250.
3 N. Shibayama, H. Ozawa, Y. Ooyama, H. Arakawa, *Bull. Chem. Soc. Jpn.* **2015**, *88*, 366.
4 S. Ida, *Bull. Chem. Soc. Jpn.* **2015**, *88*, 1619.
5 H. Kumagai, K. Takanabe, J. Kubota, K. Domen, *Bull. Chem. Soc. Jpn.* **2015**, *88*, 584.
6 M. P. Adhikari, R. Adhikari, R. G. Shrestha, R. Rajendran, L. Adhikari, P. Bairi, R. R. Pradhananga, L. K. Shrestha, K. Ariga, *Bull. Chem. Soc. Jpn.* **2015**, *88*, 1108.
7 K. Maeda, K. Domen, *Bull. Chem. Soc. Jpn.* **2016**, *89*, 627.
8 L. Wang, Y. Han, X. Feng, J. Zhou, P. Qi, B. Wang, *Coord.*

Chem. Rev. **2016**, *307*, 361.
9 K. Komori, K. Yamura, A. Kogo, Y. Takahashi, T. Tatsuma, A. Sakoda, Y. Sakai, *Bull. Chem. Soc. Jpn.* **2016**, *89*, 603.
10 Y. Tanihara, A. Nozaki, Y. Kuwahara, K. Mori, H. Yamashita, *Bull. Chem. Soc. Jpn.* **2016**, *89*, 1048.
11 V. Georgakilas, J. N. Tiwari, K. C. Kemp, J. A. Perrnan, A. B. Bourlinos, K. S. Kim, R. Zboril, *Chem. Rev.* **2016**, *116*, 5464.
12 S. E. Hosseini, M. A. Wahid, *Renewable Sustainable Energy Rev.* **2016**, *57*, 850.
13 T. Kamegawa, H. Imai, H. Yamashita, *Bull. Chem. Soc. Jpn.* **2016**, *89*, 743.
14 S. Peng, G. Jin, L. Li, K. Li, M. Srinivasan, S. Ramakrishna, J. Chen, *Chem. Soc. Rev.* **2016**, *45*, 1225.
15 H. Kataoka, T. Nakanishi, S. Omagari, Y. Takabatake, Y. Kitagawa, Y. Hasegawa, *Bull. Chem. Soc. Jpn.* **2016**, *89*, 103.
16 W. R. Erwin, H. F. Zarick, E. M. Talbert, R. Bardhan, *Energy Environ. Sci.* **2016**, *9*, 1577.
17 V. Malgras, Q. Ji, Y. Kamachi, T. Mori, F.-K. Shieh, K. C.-W. Wu, K. Ariga, Y. Yamauchi, *Bull. Chem. Soc. Jpn.* **2015**, *88*, 1171.
18 H. Liu, Z. Huang, S. Wei, L. Zheng, L. Xiao, Q. Gong, *Nanoscale* **2016**, *8*, 6209.
19 P. Bairi, K. Minami, J. P. Hill, W. Nakanishi, L. K. Shrestha, C. Liu, K. Harano, E. Nakamura, K. Ariga, *ACS Nano* **2016**, *10*, 8796.
20 K. Sakaushi, M. Antonietti, *Bull. Chem. Soc. Jpn.* **2015**, *88*, 386.
21 Z. Huang, S. Che, *Bull. Chem. Soc. Jpn.* **2015**, *88*, 617.
22 E. Yamamoto, K. Kuroda, *Bull. Chem. Soc. Jpn.* **2016**, *89*, 501.
23 H. Tabuchi, K. Urita, I. Moriguchi, *Bull. Chem. Soc. Jpn.* **2015**, *88*, 1378.
24 K. Wu, T. Lian, *Chem. Soc. Rev.* **2016**, *45*, 3781.
25 K. Ariga, M. Li, G. J. Richards, J. P. Hill, *J. Nanosci. Nanotechnol.* **2011**, *11*, 1.
26 K. Ariga, Q. Ji, J. P. Hill, Y. Bando, M. Aono, *NPG Asia Mater.* **2012**, *4*, e17.
27 K. Ariga, Q. Ji, W. Nakanishi, J. P. Hill, M. Aono, *Mater. Horiz.* **2015**, *2*, 406.
28 M. Aono, K. Ariga, *Adv. Mater.* **2016**, *28*, 989.
29 K. Ariga, K. Minami, M. Ebara, J. Nakanishi, *Polym. J.* **2016**, *48*, 371.
30 K. Ariga, *ChemNanoMat* **2016**, *2*, 333.
31 K. Ariga, M. Aono, *Jpn. J. Appl. Phys.* **2016**, *55*, 1102A6.
32 S. Hecht, *Angew. Chem., Int. Ed.* **2003**, *42*, 24.
33 K. Ariga, Y. Yamauchi, G. Rydzek, Q. Ji, Y. Yonamine, K. C.-W. Wu, J. P. Hill, *Chem. Lett.* **2014**, *43*, 36.
34 Y. Shirai, K. Minami, W. Nakanishi, Y. Yonamine, C. Joachim, K. Ariga, *Jpn. J. Appl. Phys.* **2016**, *55*, 1102A2.
35 Y. Wakayama, *Jpn. J. Appl. Phys.* **2016**, *55*, 1102AA.
36 K. Ariga, A. Vinu, Y. Yamauchi, Q. Ji, J. P. Hill, *Bull. Chem. Soc. Jpn.* **2012**, *85*, 1.
37 G. Rydzek, Q. Ji, M. Li, P. Schaaf, J. P. Hill, F. Boulmedais, K. Ariga, *Nano Today* **2015**, *10*, 138.
38 S. Cordier, F. Grasset, Y. Molard, M. Amela-Cortes, R. Boukherroub, S. Ravaine, M. Mortier, N. Ohashi, N. Saito, H. Haneda, *J. Inorg. Organomet. Polym. Mater.* **2015**, *25*, 189.
39 H. Pan, S. Zhu, L. Mao, *J. Inorg. Organomet. Polym. Mater.* **2015**, *25*, 179.
40 L. Zhang, T. Wang, Z. Shen, M. Liu, *Adv. Mater.* **2016**, *28*, 1044.
41 K. L. Wang, K. Galatsis, R. Ostroumov, A. Khitun, Z. Zhao, S. Han, *Proc. IEEE* **2008**, *96*, 212.
42 Y. J. Li, Y. Yan, Y. S. Zhao, J. Yao, *Adv. Mater.* **2016**, *28*, 1319.
43 S. Ishihara, J. Labuta, W. Van Rossom, D. Ishikawa, K. Minami, J. P. Hill, K. Ariga, *Phys. Chem. Chem. Phys.* **2014**, *16*, 9713.
44 K. Ariga, K. Minami, L. K. Shrestha, *Analyst* **2016**, *141*, 2629.
45 M. Pandeeswar, S. P. Senanayak, T. Govindaraju, *ACS Appl. Mater. Interfaces* **2016**, *8*, 30362.
46 K. Ariga, *Anal. Sci.* **2016**, *32*, 1141.
47 K. Ariga, S. Ishihara, H. Abe, M. Li, J. P. Hill, *J. Mater. Chem.* **2012**, *22*, 2369.
48 S. Jiang, L. Lv, Q. Li, J. Wang, K. Landfester, D. Crespy, *Nanoscale* **2016**, *8*, 11511.
49 C.-M. Puscasu, E. M. Seftel, M. Mertens, P. Cool, G. Carja, *J. Inorg. Organomet. Polym. Mater.* **2015**, *25*, 259.
50 K. Ariga, S. Ishihara, H. Abe, *CrystEngComm* **2016**, *18*, 6770.
51 H. Abe, J. Liu, K. Ariga, *Mater. Today* **2016**, *19*, 12.
52 K. Ariga, J. Li, J. Fei, Q. Ji, J. P. Hill, *Adv. Mater.* **2016**, *28*, 1251.
53 K. Ariga, Q. Ji, T. Mori, M. Naito, Y. Yamauchi, H. Abe, J. P. Hill, *Chem. Soc. Rev.* **2013**, *42*, 6322.
54 P. Kujawa, F. M. Winnik, *Langmuir* **2013**, *29*, 7354.
55 K. Ariga, Q. Ji, M. J. McShane, Y. M. Lvov, A. Vinu, J. P. Hill, *Chem. Mater.* **2012**, *24*, 728.
56 E. Psarra, U. König, Y. Ueda, C. Bellmann, A. Janke, E. Bittrich, K.-J. Eichhorn, P. Uhlmann, *ACS Appl. Mater. Interfaces* **2015**, *7*, 12516.
57 W. Nakanishi, K. Minami, L. K. Shrestha, Q. Ji, J. P. Hill, K. Ariga, *Nano Today* **2014**, *9*, 378.
58 R. Rajendran, L. K. Shrestha, R. M. Kumar, R. Jayavel, J. P. Hill, K. Ariga, *J. Inorg. Organomet. Polym. Mater.* **2015**, *25*, 267.
59 R. Rajendran, L. K. Shrestha, K. Minami, M. Subramanian, R. Jayavel, K. Ariga, *J. Mater. Chem. A* **2014**, *2*, 18480.
60 K. Takada, *Langmuir* **2013**, *29*, 7538.
61 K. Takada, N. Ohta, Y. Tateyama, *J. Inorg. Organomet. Polym. Mater.* **2015**, *25*, 205.
62 Q. Zou, K. Liu, M. Abbas, X. Yan, *Adv. Mater.* **2016**, *28*, 1031.
63 K. S. Novoselov, V. I. Fal'ko, L. Colombo, P. R. Gellert, M. G. Schwab, K. Kim, *Nature* **2012**, *490*, 192.
64 D. S. L. Abergel, V. Apalkov, J. Berashevich, K. Ziegler, T. Chakraborty, *Adv. Phys.* **2010**, *59*, 261.
65 M. D. Stoller, S. Park, Y. Zhu, J. An, R. S. Ruoff, *Nano Lett.* **2008**, *8*, 3498.
66 R. R. Nair, P. Blake, A. N. Grigorenko, K. S. Novoselov, T. J. Booth, T. Stauber, N. M. R. Peres, A. K. Geim, *Science* **2008**, *320*, 1308.
67 C. Lee, X. Wei, J. W. Kysar, J. Hone, *Science* **2008**, *321*, 385.
68 A. A. Balandin, S. Ghosh, W. Bao, I. Calizo, D. Teweldebrhan, F. Miao, C. N. Lau, *Nano Lett.* **2008**, *8*, 902.
69 K. S. Novoselov, A. K. Geim, S. V. Morozov, D. Jiang, Y. Zhang, S. V. Dubonos, I. V. Grigorieva, A. A. Firsov, *Science* **2004**, *306*, 666.
70 Y. Zhang, Y.-W. Tan, H. L. Stormer, P. Kim, *Nature* **2005**, *438*, 201.
71 L. A. Ponomarenko, R. V. Gorbachev, G. L. Yu, D. C. Elias,

R. Jalil, A. A. Patel, A. Mishchenko, A. S. Mayorov, C. R. Woods, J. R. Wallbank, M. Mucha-Kruczynski, B. A. Piot, M. Potemski, I. V. Grigorieva, K. S. Novoselov, F. Guinea, V. I. Fal'ko, A. K. Geim, *Nature* **2013**, *497*, 594.
72 M. Chhowalla, H. S. Shin, G. Eda, L.-J. Li, K. P. Loh, H. Zhang, *Nat. Chem.* **2013**, *5*, 263.
73 X. Huang, Z. Zeng, H. Zhang, *Chem. Soc. Rev.* **2013**, *42*, 1934.
74 M. Chhowalla, Z. Liu, H. Zhang, *Chem. Soc. Rev.* **2015**, *44*, 2584.
75 H. Zhang, *ACS Nano* **2015**, *9*, 9451.
76 C. Tan, H. Zhang, *Chem. Soc. Rev.* **2015**, *44*, 2713.
77 C. Zhi, Y. Bando, C. Tang, H. Kuwahara, D. Golberg, *Adv. Mater.* **2009**, *21*, 2889.
78 W.-J. Ong, L.-L. Tan, Y. H. Ng, S.-T. Yong, S.-P. Chai, *Chem. Rev.* **2016**, *116*, 7159.
79 M. Xu, T. Liang, M. Shi, H. Chen, *Chem. Rev.* **2013**, *113*, 3766.
80 M. Osada, T. Sasaki, *J. Mater. Chem.* **2009**, *19*, 2503.
81 Q. Wang, D. O'Hare, *Chem. Rev.* **2012**, *112*, 4124.
82 X. Huang, S. Tang, X. Mu, Y. Dai, G. Chen, Z. Zhou, F. Ruan, Z. Yang, N. Zheng, *Nat. Nanotechnol.* **2011**, *6*, 28.
83 X. Huang, S. Li, Y. Huang, S. Wu, X. Zhou, S. Li, C. L. Gan, F. Boey, C. A. Mirkin, H. Zhang, *Nat. Commun.* **2011**, *2*, 292.
84 H. Duan, N. Yan, R. Yu, C.-R. Chang, G. Zhou, H.-S. Hu, H. Rong, Z. Niu, J. Mao, H. Asakura, T. Tanaka, P. J. Dyson, J. Li, Y. Li, *Nat. Commun.* **2014**, *5*, 3093.
85 Z. Fan, X. Huang, C. Tan, H. Zhang, *Chem. Sci.* **2015**, *6*, 95.
86 Y. Peng, Y. Li, Y. Ban, H. Jin, W. Jiao, X. Liu, W. Yang, *Science* **2014**, *346*, 1356.
87 T. Rodenas, I. Luz, G. Prieto, B. Seoane, H. Miro, A. Corma, F. Kapteijn, F. X. Llabrés i Xamena, J. Gascon, *Nat. Mater.* **2015**, *14*, 48.
88 J. W. Colson, A. R. Woll, A. Mukherjee, M. P. Levendorf, E. L. Spitler, V. B. Shields, M. G. Spencer, J. Park, W. R. Dichtel, *Science* **2011**, *332*, 228.
89 M. J. Kory, M. Wörle, T. Weber, P. Payamyar, S. W. van de Poll, J. Dshemuchadse, N. Trapp, A. D. Schlüter, *Nat. Chem.* **2014**, *6*, 779.
90 P. Kissel, D. J. Murray, W. J. Wulftange, V. J. Catalano, B. T. King, *Nat. Chem.* **2014**, *6*, 774.
91 M. Naguib, V. N. Mochalin, M. W. Barsoum, Y. Gogotsi, *Adv. Mater.* **2014**, *26*, 992.
92 H. Liu, Y. Du, Y. Deng, P. D. Ye, *Chem. Soc. Rev.* **2015**, *44*, 2732.
93 B. Lalmi, H. Oughaddou, H. Enriquez, A. Kara, S. Vizzini, B. Ealet, B. Aufray, *Appl. Phys. Lett.* **2010**, *97*, 223109.
94 A. K. Geim, K. S. Novoselov, *Nat. Mater.* **2007**, *6*, 183.
95 K. R. Paton, E. Varrla, C. Backes, R. J. Smith, U. Khan, A. O'Neill, C. Boland, M. Lotya, O. M. Istrate, P. King, T. Higgins, S. Barwich, P. May, P. Puczkarski, I. Ahmed, M. Moebius, H. Pettersson, E. Long, J. Coelho, S. E. O'Brien, E. K. McGuire, B. M. Sanchez, G. S. Duesberg, N. McEvoy, T. J. Pennycook, C. Downing, A. Crossley, V. Nicolosi, J. N. Coleman, *Nat. Mater.* **2014**, *13*, 624.
96 K. S. Novoselov, D. Jiang, F. Schedin, T. J. Booth, V. V. Khotkevich, S. V. Morozov, A. K. Geim, *Proc. Natl. Acad. Sci. U.S.A.* **2005**, *102*, 10451.
97 V. Goyal, D. Teweldebrhan, A. A. Balandin, *Appl. Phys. Lett.* **2010**, *97*, 133117.
98 C. R. Dean, A. F. Young, I. Meric, C. Lee, L. Wang, S. Sorgenfrei, K. Watanabe, T. Taniguchi, P. Kim, K. L. Shepard, J. Hone, *Nat. Nanotechnol.* **2010**, *5*, 722.
99 H. Li, Z. Yin, Q. He, H. Li, X. Huang, G. Lu, D. W. H. Fam, A. I. Y. Tok, Q. Zhang, H. Zhang, *Small* **2012**, *8*, 63.
100 H. Li, G. Lu, Y. Wang, Z. Yin, C. Cong, Q. He, L. Wang, F. Ding, T. Yu, H. Zhang, *Small* **2013**, *9*, 1974.
101 A. Castellanos-Gomez, L. Vicarelli, E. Prada, J. O. Island, K. L. Narasimha-Acharya, S. I. Blanter, D. J. Groenendijk, M. Buscema, G. A. Steele, J. V. Alvarez, H. W. Zandbergen, J. J. Palacios, H. S. J. van der Zant, *2D Mater.* **2014**, *1*, 025001.
102 H. Li, J. Wu, Z. Yin, H. Zhang, *Acc. Chem. Res.* **2014**, *47*, 1067.
103 Y. Hernandez, V. Nicolosi, M. Lotya, F. M. Blighe, Z. Sun, S. De, I. T. McGovern, B. Holland, M. Byrne, Y. K. Gun'Ko, J. J. Boland, P. Niraj, G. Duesberg, S. Krishnamurthy, R. Goodhue, J. Hutchison, V. Scardaci, A. C. Ferrari, J. N. Coleman, *Nat. Nanotechnol.* **2008**, *3*, 563.
104 J. N. Coleman, M. Lotya, A. O'Neill, S. D. Bergin, P. J. King, U. Khan, K. Young, A. Gaucher, S. De, R. J. Smith, I. V. Shvets, S. K. Arora, G. Stanton, H.-Y. Kim, K. Lee, G. T. Kim, G. S. Duesberg, T. Hallam, J. J. Boland, J. J. Wang, J. F. Donegan, J. C. Grunlan, G. Moriarty, A. Shmeliov, R. J. Nicholls, J. M. Perkins, E. M. Grieveson, K. Theuwissen, D. W. McComb, P. D. Nellist, V. Nicolosi, *Science* **2011**, *331*, 568.
105 U. Khan, P. May, A. O'Neill, A. P. Bell, E. Boussac, A. Martin, J. Semple, J. N. Coleman, *Nanoscale* **2013**, *5*, 581.
106 V. Nicolosi, M. Chhowalla, M. G. Kanatzidis, M. S. Strano, J. N. Coleman, *Science* **2013**, *340*, 1226419.
107 D. Hanlon, C. Backes, T. M. Higgins, M. Hughes, A. O'Neill, P. King, N. McEvoy, G. S. Duesberg, B. M. Sanchez, H. Pettersson, V. Nicolosi, J. N. Coleman, *Chem. Mater.* **2014**, *26*, 1751.
108 J. R. Brent, N. Savjani, E. A. Lewis, S. J. Haigh, D. J. Lewis, P. O'Brien, *Chem. Commun.* **2014**, *50*, 13338.
109 L. Liang, K. Li, C. Xiao, S. Fan, J. Liu, W. Zhang, W. Xu, W. Tong, J. Liao, Y. Zhou, B. Ye, Y. Xie, *J. Am. Chem. Soc.* **2015**, *137*, 3102.
110 M. B. Dines, *Mater. Res. Bull.* **1975**, *10*, 287.
111 P. Joensen, R. F. Frindt, S. R. Morrison, *Mater. Res. Bull.* **1986**, *21*, 457.
112 L. M. Viculis, J. J. Mack, O. M. Mayer, H. T. Hahn, R. B. Kaner, *J. Mater. Chem.* **2005**, *15*, 974.
113 Z. Zeng, Z. Yin, X. Huang, H. Li, Q. He, G. Lu, F. Boey, H. Zhang, *Angew. Chem., Int. Ed.* **2011**, *50*, 11093.
114 Z. Zeng, T. Sun, J. Zhu, X. Huang, Z. Yin, G. Lu, Z. Fan, Q. Yan, H. H. Hng, H. Zhang, *Angew. Chem., Int. Ed.* **2012**, *51*, 9052.
115 Z. Zeng, C. Tan, X. Huang, S. Bao, H. Zhang, *Energy Environ. Sci.* **2014**, *7*, 797.
116 J. Zhang, H. Zhang, S. Dong, Y. Liu, C. T. Nai, H. S. Shin, H. Y. Jeong, B. Liu, K. P. Loh, *Nat. Commun.* **2014**, *5*, 2995.
117 K. Parvez, Z.-S. Wu, R. Li, X. Liu, R. Graf, X. Feng, K. Müllen, *J. Am. Chem. Soc.* **2014**, *136*, 6083.
118 J. Shen, Y. Zhu, H. Jiang, C. Li, *Nano Today* **2016**, *11*, 483.
119 A. Castellanos-Gomez, M. Barkelid, A. M. Goossens, V. E. Calado, H. S. J. van der Zant, G. A. Steele, *Nano Lett.* **2012**, *12*, 3187.
120 X. Li, W. Cai, J. An, S. Kim, J. Nah, D. Yang, R. Piner, A. Velamakanni, I. Jung, E. Tutuc, S. K. Banerjee, L. Colombo, R. S. Ruoff, *Science* **2009**, *324*, 1312.
121 L. Song, L. Ci, H. Lu, P. B. Sorokin, C. Jin, J. Ni, A. G. Kvashnin, D. G. Kvashnin, J. Lou, B. I. Yakobson, P. M. Ajayan,

Nano Lett. **2010**, *10*, 3209.
122 Y.-H. Lee, X.-Q. Zhang, W. Zhang, M.-T. Chang, C.-T. Lin, K.-D. Chang, Y.-C. Yu, J. T.-W. Wang, C.-S. Chang, L.-J. Li, T.-W. Lin, *Adv. Mater.* **2012**, *24*, 2320.
123 Q. Ji, Y. Zhang, Y. Zhang, Z. Liu, *Chem. Soc. Rev.* **2015**, *44*, 2587.
124 Y. Shi, H. Li, L.-J. Li, *Chem. Soc. Rev.* **2015**, *44*, 2744.
125 D. Yoo, M. Kim, S. Jeong, J. Han, J. Cheon, *J. Am. Chem. Soc.* **2014**, *136*, 14670.
126 Z. Fan, X. Huang, Y. Han, M. Bosman, Q. Wang, Y. Zhu, Q. Liu, B. Li, Z. Zeng, J. Wu, W. Shi, S. Li, C. L. Gan, H. Zhang, *Nat. Commun.* **2015**, *6*, 6571.
127 S. Gao, Y. Sun, F. Lei, L. Liang, J. Liu, W. Bi, B. Pan, Y. Xie, *Angew. Chem., Int. Ed.* **2014**, *53*, 12789.
128 Z. Sun, T. Liao, Y. Dou, S. M. Hwang, M.-S. Park, L. Jiang, J. H. Kim, S. X. Dou, *Nat. Commun.* **2014**, *5*, 3813.
129 S. Acharya, B. Das, U. Thupakula, K. Ariga, D. D. Sarma, J. Israelachvili, Y. Golan, *Nano Lett.* **2013**, *13*, 409.
130 Y. Sun, Z. Sun, S. Gao, H. Cheng, Q. Liu, J. Piao, T. Yao, C. Wu, S. Hu, S. Wei, Y. Xie, *Nat. Commun.* **2012**, *3*, 1057.
131 C. L. Tan, H. Zhang, *Nat. Commun.* **2015**, *6*, 7873.
132 A. K. Geim, *Science* **2009**, *324*, 1530.
133 J. Wu, W. Pisula, K. Müllen, *Chem. Rev.* **2007**, *107*, 718.
134 F. Guinea, M. I. Katsnelson, A. K. Geim, *Nat. Phys.* **2010**, *6*, 30.
135 C. E. Banks, R. R. Moore, T. J. Davies, R. G. Compton, *Chem. Commun.* **2004**, *21*, 1804.
136 W. Li, C. Tan, M. A. Lowe, H. D. Abruña, D. C. Ralph, *ACS Nano* **2011**, *5*, 2264.
137 D. K. Kampouris, C. E. Banks, *Chem. Commun.* **2010**, *46*, 8986.
138 P. Blake, P. D. Brimicombe, R. R. Nair, T. J. Booth, D. Jiang, F. Schedin, L. A. Ponomarenko, S. V. Morozov, H. F. Gleeson, E. W. Hill, A. K. Geim, K. S. Novoselov, *Nano Lett.* **2008**, *8*, 1704.
139 Y. Hernandez, M. Lotya, D. Rickard, S. D. Bergin, J. N. Coleman, *Langmuir* **2010**, *26*, 3208.
140 M. Lotya, P. J. King, U. Khan, S. De, J. N. Coleman, *ACS Nano* **2010**, *4*, 3155.
141 J. M. Englert, J. Röhrl, C. D. Schmidt, R. Graupner, M. Hundhausen, F. Hauke, A. Hirsch, *Adv. Mater.* **2009**, *21*, 4265.
142 D. A. C. Brownson, J. P. Metters, D. K. Kampouris, C. E. Banks, *Electroanalysis* **2011**, *23*, 894.
143 X. Li, G. Zhang, X. Bai, X. Sun, X. Wang, E. Wang, H. Dai, *Nat. Nanotechnol.* **2008**, *3*, 538.
144 C. Vallés, C. Drummond, H. Saadaoui, C. A. Furtado, M. He, O. Roubeau, L. Ortolani, M. Monthioux, A. Pénicaud, *J. Am. Chem. Soc.* **2008**, *130*, 15802.
145 N. Behabtu, J. R. Lomeda, M. J. Green, A. L. Higginbotham, A. Sinitskii, D. V. Kosynkin, D. Tsentalovich, A. N. G. Parra-Vasquez, J. Schmidt, E. Kesselman, Y. Cohen, Y. Talmon, J. M. Tour, M. Pasquali, *Nat. Nanotechnol.* **2010**, *5*, 406.
146 Y. Takada, R. Fujii, *Tanso* **1985**, 110.
147 A. Jnioui, A. Metrot, A. Storck, *Electrochim. Acta* **1982**, *27*, 1247.
148 C. T. J. Low, F. C. Walsh, M. H. Chakrabarti, M. A. Hashim, M. A. Hussain, *Carbon* **2013**, *54*, 1.
149 C.-Y. Su, A.-Y. Lu, Y. Xu, F.-R. Chen, A. N. Khlobystov, L.-J. Li, *ACS Nano* **2011**, *5*, 2332.
150 G. Wang, B. Wang, J. Park, Y. Wang, B. Sun, J. Yao, *Carbon* **2009**, *47*, 3242.
151 M. Alanyalıoğlu, J. J. Segura, J. Oró-Solè, N. Casañ-Pastor, *Carbon* **2012**, *50*, 142.
152 G. M. Morales, P. Schifani, G. Ellis, C. Ballesteros, G. Martínez, C. Barbero, H. J. Salavagione, *Carbon* **2011**, *49*, 2809.
153 Y. L. Zhong, T. M. Swager, *J. Am. Chem. Soc.* **2012**, *134*, 17896.
154 D. Voiry, A. Mohite, M. Chhowalla, *Chem. Soc. Rev.* **2015**, *44*, 2702.
155 D. R. Dreyer, R. S. Ruoff, C. W. Bielawski, *Angew. Chem., Int. Ed.* **2010**, *49*, 9336.
156 D. R. Dreyer, S. Park, C. W. Bielawski, R. S. Ruoff, *Chem. Soc. Rev.* **2010**, *39*, 228.
157 M. J. Allen, V. C. Tung, R. B. Kaner, *Chem. Rev.* **2010**, *110*, 132.
158 W. Hummers, Jr., R. E. Offeman, *J. Am. Chem. Soc.* **1958**, *80*, 1339.
159 Y. Zhu, S. Murali, W. Cai, X. Li, J. W. Suk, J. R. Potts, R. S. Ruoff, *Adv. Mater.* **2010**, *22*, 3906.
160 X. Huang, X. Qi, F. Boey, H. Zhang, *Chem. Soc. Rev.* **2012**, *41*, 666.
161 C. Tan, X. Huang, H. Zhang, *Mater. Today* **2013**, *16*, 29.
162 A. Ambrosi, C. K. Chua, A. Bonanni, M. Pumera, *Chem. Rev.* **2014**, *114*, 7150.
163 X. Huang, C. Tan, Z. Yin, H. Zhang, *Adv. Mater.* **2014**, *26*, 2185.
164 T. Kuilla, S. Bhadra, D. Yao, N. H. Kim, S. Bose, J. H. Lee, *Prog. Polym. Sci.* **2010**, *35*, 1350.
165 A. Ambrosi, C. K. Chua, N. M. Latiff, A. H. Loo, C. H. A. Wong, A. Y. S. Eng, A. Bonanni, M. Pumera, *Chem. Soc. Rev.* **2016**, *45*, 2458.
166 Y. Zhang, Y. Zhang, Q. Ji, J. Ju, H. Yuan, J. Shi, T. Gao, D. Ma, M. Liu, Y. Chen, X. Song, H. Y. Hwang, Y. Cui, Z. Liu, *ACS Nano* **2013**, *7*, 8963.
167 Q. Zhang, E. Uchaker, S. L. Candelaria, G. Cao, *Chem. Soc. Rev.* **2013**, *42*, 3127.
168 P. Ro. Bueno, C. Gabrielli, *Electrochemistry, Nanomaterials, and Nanostructures*, in *Nanostructured Materials Electrochemical Energy Production and Storage*, ed. by E. R. Leite, Springer, **2009**, Chap. 3, pp. 81–150. doi:10.1007/978-0-387-49323-7_3.
169 S. Ghosh, T. Maiyalagan, R. N. Basu, *Nanoscale* **2016**, *8*, 6921.
170 S. P. S. Badwal, S. Giddey, A. Kulkarni, J. Goel, S. Basu, *Appl. Energy* **2015**, *145*, 80.
171 Y. Holade, C. Morais, K. Servat, T. W. Napporn, K. B. Kokoh, *ACS Catal.* **2013**, *3*, 2403.
172 S. Ghosh, A.-L. Teillout, D. Floresyona, P. de Oliveira, A. Hagège, H. Remita, *Int. J. Hydrogen Energy* **2015**, *40*, 4951.
173 W. Vielstich, A. Lamm, H. A. Gasteiger, *Handbook of Fuel Cells: Fundamentals, Technology, Applications*, Wiley, New York, **2003**. doi:10.1002/9780470974001.
174 M. Liu, R. Zhang, W. Chen, *Chem. Rev.* **2014**, *114*, 5117.
175 S. Sardar, S. Ghosh, H. Remita, P. Kar, B. Liu, C. Bhattacharya, P. Lemmens, S. K. Pal, *RSC Adv.* **2016**, *6*, 33433.
176 B. Seger, P. V. Kamat, *J. Phys. Chem. C* **2009**, *113*, 7990.
177 E. Yoo, T. Okata, T. Akita, M. Kohyama, J. Nakamura, I. Honma, *Nano Lett.* **2009**, *9*, 2255.
178 P. Kar, S. Sardar, B. Liu, M. Sreemany, P. Lemmens, S. Ghosh, S. K. Pal, *Sci. Technol. Adv. Mater.* **2016**, *17*, 375.
179 Z. Jin, D. Nackashi, W. Lu, C. Kittrell, J. M. Tour, *Chem. Mater.* **2010**, *22*, 5695.
180 S. Guo, S. Dong, E. Wang, *ACS Nano* **2010**, *4*, 547.
181 L. Dong, R. R. S. Gari, Z. Li, M. M. Craig, S. Hou, *Carbon*

2010, *48*, 781.
182 S. Zhang, Y. Shao, H. Liao, M. H. Engelhard, G. Yin, Y. Lin, *ACS Nano* **2011**, *5*, 1785.
183 S. Stankovich, D. A. Dikin, G. H. B. Dommett, K. M. Kohlhaas, E. J. Zimney, E. A. Stach, R. D. Piner, S. T. Nguyen, R. S. Ruoff, *Nature* **2006**, *442*, 282.
184 C. N. R. Rao, A. K. Sood, K. S. Subrahmanyam, *Angew. Chem., Int. Ed.* **2009**, *48*, 7752.
185 X. Du, I. Skachko, A. Barker, E. Y. Andrei, *Nat. Nanotechnol.* **2008**, *3*, 491.
186 Y. Liang, Y. Li, H. Wang, J. Zhou, J. Wang, T. Regier, H. Dai, *Nat. Mater.* **2011**, *10*, 780.
187 R. Kou, Y. Shao, D. Mei, Z. Nie, D. Wang, C. Wang, V. V. Viswanathan, S. Park, I. A. Aksay, Y. Lin, Y. Wang, J. Liu, *J. Am. Chem. Soc.* **2011**, *133*, 2541.
188 S. Ghosh, H. Remita, P. Kar, S. Choudhury, S. Sardar, P. Beaunier, P. S. Roy, S. K. Bhattacharya, S. K. Pal, *J. Mater. Chem. A* **2015**, *3*, 9517.
189 S. I. Shin, A. Go, I. Y. Kim, J. M. Lee, Y. Lee, S.-J. Hwang, *Energy Environ. Sci.* **2013**, *6*, 608.
190 D. Wang, D. Choi, J. Li, Z. Yang, Z. Nie, R. Kou, D. Hu, C. Wang, L. V. Saraf, J. Zhang, I. A. Aksay, J. Liu, *ACS Nano* **2009**, *3*, 907.
191 S.-M. Paek, E. Yoo, I. Honma, *Nano Lett.* **2009**, *9*, 72.
192 G. Goncalves, P. A. A. P. Marques, C. M. Granadeiro, H. I. S. Nogueira, M. K. Singh, J. Grácio, *Chem. Mater.* **2009**, *21*, 4796.
193 C. Xu, X. Wang, J. Zhu, *J. Phys. Chem. C* **2008**, *112*, 19841.
194 S. Ghosh, Y. Holade, H. Remita, K. Servat, P. Beaunier, A. Hagège, K. B. Kokoh, T. W. Napporn, *Electrochim. Acta* **2016**, *212*, 864.
195 K. Gong, F. Du, Z. Xia, M. Durstock, L. Dai, *Science* **2009**, *323*, 760.
196 H. Wang, Z. Lu, D. Kong, J. Sun, T. M. Hymel, Y. Cui, *ACS Nano* **2014**, *8*, 4940.
197 Y. Zhao, R. Nakamura, K. Kamiya, S. Nakanishi, K. Hashimoto, *Nat. Commun.* **2013**, *4*, 2390.
198 Y. Liu, H. Jiang, Y. Zhu, X. Yang, C. Li, *J. Mater. Chem. A* **2016**, *4*, 1694.
199 M. Jahan, Z. Liu, K. P. Loh, *Adv. Funct. Mater.* **2013**, *23*, 5363.
200 D. Higgins, P. Zamani, A. Yu, Z. Chen, *Energy Environ. Sci.* **2016**, *9*, 357.
201 L. Tao, Q. Wang, S. Dou, Z. Ma, J. Huo, S. Wang, L. Dai, *Chem. Commun.* **2016**, *52*, 2764.
202 L. Dai, Y. Xue, L. Qu, H.-J. Choi, J.-B. Baek, *Chem. Rev.* **2015**, *115*, 4823.
203 D. Deng, L. Yu, X. Pan, S. Wang, X. Chen, P. Hu, L. Sun, X. Bao, *Chem. Commun.* **2011**, *47*, 10016.
204 I.-Y. Jeon, D. Yu, S.-Y. Bae, H.-J. Choi, D. W. Chang, L. Dai, J.-B. Baek, *Chem. Mater.* **2011**, *23*, 3987.
205 Y. Gong, H. Fei, X. Zou, W. Zhou, S. Yang, G. Ye, Z. Liu, Z. Peng, J. Lou, R. Vajtai, B. I. Yakobson, J. M. Tour, P. M. Ajayan, *Chem. Mater.* **2015**, *27*, 1181.
206 S. M. Lyth, Y. Nabae, S. Moriya, S. Kuroki, M. Kakimoto, J. Ozaki, S. Miyata, *J. Phys. Chem. C* **2009**, *113*, 20148.
207 S. Yang, X. Feng, X. Wang, K. Müllen, *Angew. Chem., Int. Ed.* **2011**, *50*, 5339.
208 Y. Zheng, Y. Jiao, J. Chen, J. Liu, J. Liang, A. Du, W. Zhang, Z. Zhu, S. Smith, M. Jaroniec, G. Q. Lu, S. Z. Qiao, *J. Am. Chem. Soc.* **2011**, *133*, 20116.
209 M. Shao, Q. Chang, J.-P. Dodelet, R. Chenitz, *Chem. Rev.* **2016**, *116*, 3594.
210 J. Wu, H. Yang, *Acc. Chem. Res.* **2013**, *46*, 1848.
211 J. Zhang, Z. Zhao, Z. Xia, L. Dai, *Nat. Nanotechnol.* **2015**, *10*, 444.
212 J. Jung, H. Y. Jeong, J.-S. Lee, M. G. Kim, J. Cho, *Angew. Chem., Int. Ed.* **2014**, *53*, 4582.
213 Y. Lee, J. Suntivich, K. J. May, E. E. Perry, Y. Shao-Horn, *J. Phys. Chem. Lett.* **2012**, *3*, 399.
214 S. Ghosh, P. Kar, N. Bhandary, S. Basu, S. Sardar, T. Maiyalagan, D. Majumdar, S. K. Bhattacharya, A. Bhaumik, P. Lemmens, S. K. Pal, *Catal. Sci. Technol.* **2016**, *6*, 1417.
215 Y. Zheng, Y. Jiao, Y. Zhu, L. H. Li, Y. Han, Y. Chen, A. Du, M. Jaroniec, S. Z. Qiao, *Nat. Commun.* **2014**, *5*, 3783.
216 T. Y. Ma, S. Dai, M. Jaroniec, S. Z. Qiao, *Angew. Chem., Int. Ed.* **2014**, *53*, 7281.
217 S. J. Rowley-Neale, D. A. C. Brownson, G. C. Smith, D. A. G. Sawtell, P. J. Kelly, C. E. Banks, *Nanoscale* **2015**, *7*, 18152.
218 M. A. Lukowski, A. S. Daniel, F. Meng, A. Forticaux, L. Li, S. Jin, *J. Am. Chem. Soc.* **2013**, *135*, 10274.
219 D. Voiry, M. Salehi, R. Silva, T. Fujita, M. Chen, T. Asefa, V. B. Shenoy, G. Eda, M. Chhowalla, *Nano Lett.* **2013**, *13*, 6222.
220 T. F. Jaramillo, K. P. Jørgensen, J. Bonde, J. H. Nielsen, S. Horch, I. Chorkendorff, *Science* **2007**, *317*, 100.
221 D. R. Cummins, U. Martinez, A. Sherehiy, R. Kappera, A. Martinez-Garcia, R. K. Schulze, J. Jasinski, J. Zhang, R. K. Gupta, J. Lou, M. Chhowalla, G. Sumanasekera, A. D. Mohite, M. K. Sunkara, G. Gupta, *Nat. Commun.* **2016**, *7*, 11857.
222 D. Voiry, H. Yamaguchi, J. Li, R. Silva, D. C. B. Alves, T. Fujita, M. Chen, T. Asefa, V. B. Shenoy, G. Eda, M. Chhowalla, *Nat. Mater.* **2013**, *12*, 850.
223 X. J. Chua, J. Luxa, A. Y. S. Eng, S. M. Tan, Z. Sofer, M. Pumera, *ACS Catal.* **2016**, *6*, 5724.
224 L. Liao, J. Zhu, X. Bian, L. Zhu, M. D. Scanlon, H. H. Girault, B. Liu, *Adv. Funct. Mater.* **2013**, *23*, 5326.
225 Y. Li, H. Wang, L. Xie, Y. Liang, G. Hong, H. Dai, *J. Am. Chem. Soc.* **2011**, *133*, 7296.
226 Z. Chen, D. Cummins, B. N. Reinecke, E. Clark, M. K. Sunkara, T. F. Jaramillo, *Nano Lett.* **2011**, *11*, 4168.
227 T. Wang, L. Liu, Z. Zhu, P. Papakonstantinou, J. Hu, H. Liu, M. Li, *Energy Environ. Sci.* **2013**, *6*, 625.
228 M.-R. Gao, W.-T. Yao, H.-B. Yao, S.-H. Yu, *J. Am. Chem. Soc.* **2009**, *131*, 7486.
229 M.-R. Gao, Y.-F. Xu, J. Jiang, Y.-R. Zheng, S.-H. Yu, *J. Am. Chem. Soc.* **2012**, *134*, 2930.
230 M.-R. Gao, Q. Gao, J. Jiang, C.-H. Cui, W.-T. Yao, S.-H. Yu, *Angew. Chem., Int. Ed.* **2011**, *50*, 4905.
231 M.-R. Gao, S. Liu, J. Jiang, C.-H. Cui, W.-T. Yao, S.-H. Yu, *J. Mater. Chem.* **2010**, *20*, 9355.
232 M.-R. Gao, J. Jiang, S.-H. Yu, *Small* **2012**, *8*, 13.
233 M.-R. Gao, Y.-F. Xu, J. Jiang, S.-H. Yu, *Chem. Soc. Rev.* **2013**, *42*, 2986.
234 D. Merki, X. Hu, *Energy Environ. Sci.* **2011**, *4*, 3878.
235 D. Kong, J. J. Cha, H. Wang, H. R. Lee, Y. Cui, *Energy Environ. Sci.* **2013**, *6*, 3553.
236 M.-R. Gao, J.-X. Liang, Y.-R. Zheng, Y.-F. Xu, J. Jiang, Q. Gao, J. Li, S.-H. Yu, *Nat. Commun.* **2015**, *6*, 5982.
237 J. Deng, H. Li, J. Xiao, Y. Tu, D. Deng, H. Yang, H. Tian, J. Li, P. Ren, X. Bao, *Energy Environ. Sci.* **2015**, *8*, 1594.
238 J. Yang, D. Voiry, S. J. Ahn, D. Kang, A. Y. Kim, M. Chhowalla, H. S. Shin, *Angew. Chem., Int. Ed.* **2013**, *52*, 13751.

239 X. Cai, T. C. Ozawa, A. Funatsu, R. Ma, Y. Ebina, T. Sasaki, *J. Am. Chem. Soc.* **2015**, *137*, 2844.
240 J.-M. Tarascon, M. Armand, *Nature* **2001**, *414*, 359.
241 P. Simon, Y. Gogotsi, *Nat. Mater.* **2008**, *7*, 845.
242 H. Wang, Z. Xu, H. Yi, H. Wei, Z. Guo, X. Wang, *Nano Energy* **2014**, *7*, 86.
243 Y. Zhu, S. Murali, M. D. Stoller, K. J. Ganesh, W. Cai, P. J. Ferreira, A. Pirkle, R. M. Wallace, K. A. Cychosz, M. Thommes, D. Su, E. A. Stach, R. S. Ruoff, *Science* **2011**, *332*, 1537.
244 X. Peng, L. Peng, C. Wu, Y. Xie, *Chem. Soc. Rev.* **2014**, *43*, 3303.
245 L. Peng, Y. Zhu, H. Li, G. Yu, *Small* **2016**, *12*, 6183.
246 L. Peng, Y. Zhu, D. Chen, R. S. Ruoff, G. Yu, *Adv. Energy Mater.* **2016**, *6*, 1600025.
247 D. Chen, H. Feng, J. Li, *Chem. Rev.* **2012**, *112*, 6027.
248 S. Han, D. Wu, S. Li, F. Zhang, X. Feng, *Small* **2013**, *9*, 1173.
249 C. Xu, B. Xu, Y. Gu, Z. Xiong, J. Sun, X. S. Zhao, *Energy Environ. Sci.* **2013**, *6*, 1388.
250 S. Han, D. Wu, S. Li, F. Zhang, X. Feng, *Adv. Mater.* **2014**, *26*, 849.
251 X. Yang, C. Cheng, Y. Wang, L. Qiu, D. Li, *Science* **2013**, *341*, 534.
252 M. F. El-Kady, V. Strong, S. Dubin, R. B. Kaner, *Science* **2012**, *335*, 1326.
253 S. Yang, X. Feng, L. Wang, K. Tang, J. Maier, K. Müllen, *Angew. Chem., Int. Ed.* **2010**, *49*, 4795.
254 S. Yang, X. Feng, K. Müllen, *Adv. Mater.* **2011**, *23*, 3575.
255 Y. Wang, J. Guo, T. Wang, J. Shao, D. Wang, Y.-W. Yang, *Nanomaterials* **2015**, *5*, 1667.
256 W. Shi, J. Zhu, D. H. Sim, Y. Y. Tay, Z. Lu, X. Zhang, Y. Sharma, M. Srinivasan, H. Zhang, H. H. Hng, Q. Yan, *J. Mater. Chem.* **2011**, *21*, 3422.
257 Z. Wang, L. Ma, W. Chen, G. Huang, D. Chen, L. Wang, J. Y. Lee, *RSC Adv.* **2013**, *3*, 21675.
258 G. Huang, T. Chen, W. Chen, Z. Wang, K. Chang, L. Ma, F. Huang, D. Chen, J. Y. Lee, *Small* **2013**, *9*, 3693.
259 L. Ma, X. Zhou, L. Xu, X. Xu, L. Zhang, W. Chen, *J. Power Sources* **2015**, *285*, 274.
260 L. Ma, J. Ye, W. Chen, J. Wang, R. Liu, J. Y. Lee, *ChemElectroChem* **2015**, *2*, 538.
261 H. Hwang, H. Kim, J. Cho, *Nano Lett.* **2011**, *11*, 4826.
262 W. Qian, Z. Chen, S. Cottingham, W. A. Merrill, N. A. Swartz, A. M. Goforth, T. L. Clare, J. Jiao, *Green Chem.* **2012**, *14*, 371.
263 Y. Sun, S. Gao, Y. Xie, *Chem. Soc. Rev.* **2014**, *43*, 530.
264 L. Wang, C. Lin, F. Zhang, J. Jin, *ACS Nano* **2014**, *8*, 3724.
265 X. Gu, W. Cui, H. Li, Z. Wu, Z. Zeng, S.-T. Lee, H. Zhang, B. Sun, *Adv. Energy Mater.* **2013**, *3*, 1262.
266 M. R. Lukatskaya, O. Mashtalir, C. E. Ren, Y. Dall'Agnese, P. Rozier, P. L. Taberna, M. Naguib, P. Simon, M. W. Barsoum, Y. Gogotsi, *Science* **2013**, *341*, 1502.
267 C. Wu, X. Lu, L. Peng, K. Xu, X. Peng, J. Huang, G. Yu, Y. Xie, *Nat. Commun.* **2013**, *4*, 2431.
268 L. Cao, S. Yang, W. Gao, Z. Liu, Y. Gong, L. Ma, G. Shi, S. Lei, Y. Zhang, S. Zhang, R. Vajtai, P. M. Ajayan, *Small* **2013**, *9*, 2905.
269 Y. Yang, H. Fei, G. Ruan, C. Xiang, J. M. Tour, *Adv. Mater.* **2014**, *26*, 8163.
270 K. Krishnamoorthy, G. Veerasubramani, S. Radhakrishnan, S. J. Kim, *Mater. Res. Bull.* **2014**, *50*, 499.
271 A. Ramadoss, T. Kim, G.-S. Kim, S. J. Kim, *New J. Chem.* **2014**, *38*, 2379.
272 M. Acerce, D. Voiry, M. Chhowalla, *Nat. Nanotechnol.* **2015**, *10*, 313.
273 C. Wang, W. Wan, Y. Huang, J. Chen, H. H. Zhou, X. X. Zhang, *Nanoscale* **2014**, *6*, 5351.
274 Z. Wan, J. Shao, J. Yun, H. Zheng, T. Gao, M. Shen, Q. Qu, H. Zheng, *Small* **2014**, *10*, 4975.
275 L. Zhang, X. W. D. Lou, *Chem.—Eur. J.* **2014**, *20*, 5219.
276 K. Chang, W. Chen, *ACS Nano* **2011**, *5*, 4720.
277 J. Wang, J. Liu, D. Chao, J. Yan, J. Lin, Z. X. Shen, *Adv. Mater.* **2014**, *26*, 7162.
278 Y. Liu, Y. Zhao, L. Jiao, J. Chen, *J. Mater. Chem. A* **2014**, *2*, 13109.
279 Y. Teng, H. Zhao, Z. Zhang, Z. Li, Q. Xia, Y. Zhang, L. Zhao, X. Du, Z. Du, P. Lv, K. Świerczek, *ACS Nano* **2016**, *10*, 8526.
280 H. Tang, J. Wang, H. Yin, H. Zhao, D. Wang, Z. Tang, *Adv. Mater.* **2015**, *27*, 1117.
281 K. Gopalakrishnan, S. Sultan, A. Govindaraj, C. N. R. Rao, *Nano Energy* **2015**, *12*, 52.
282 L.-Q. Mai, A. Minhas-Khan, X. Tian, K. Hercule, Y.-L. Zhao, X. Lin, X. Xu, *Nat. Commun.* **2013**, *4*, 2923.
283 J. Ren, W. Bai, G. Guan, Y. Zhang, H. Peng, *Adv. Mater.* **2013**, *25*, 5965.
284 D. H. Seo, Z. J. Han, S. Kumar, K. Ostrikov, *Adv. Energy Mater.* **2013**, *3*, 1316.
285 J. Zhong, Z. Yang, R. Mukherjee, A. V. Thomas, K. Zhu, P. Sun, J. Lian, H. Zhu, N. Koratkar, *Nano Energy* **2013**, *2*, 1025.
286 Z. Ling, C. E. Ren, M.-Q. Zhao, J. Yang, J. M. Giammarco, J. Qiu, M. W. Barsoum, Y. Gogotsi, *Proc. Natl. Acad. Sci. U.S.A.* **2014**, *111*, 16676.
287 W. Luo, F. Shen, C. Bommier, H. Zhu, X. Ji, L. Hu, *Acc. Chem. Res.* **2016**, *49*, 231.
288 Z. Hu, L. Wang, K. Zhang, J. Wang, F. Cheng, Z. Tao, J. Chen, *Angew. Chem., Int. Ed.* **2014**, *126*, 13008.
289 S. D. Lacey, J. Wan, A. v. W. Cresce, S. M. Russell, J. Dai, W. Bao, K. Xu, L. Hu, *Nano Lett.* **2015**, *15*, 1018.
290 X. Xiong, W. Luo, X. Hu, C. Chen, L. Qie, D. Hou, Y. Huang, *Sci. Rep.* **2015**, *5*, 9254.
291 C. Zhu, X. Mu, P. A. van Aken, Y. Yu, J. Maier, *Angew. Chem., Int. Ed.* **2014**, *53*, 2152.
292 S. H. Choi, Y. N. Ko, J.-K. Lee, Y. C. Kang, *Adv. Funct. Mater.* **2015**, *25*, 1780.
293 L. David, R. Bhandavat, G. Singh, *ACS Nano* **2014**, *8*, 1759.
294 X. Xie, Z. Ao, D. Su, J. Zhang, G. Wang, *Adv. Funct. Mater.* **2015**, *25*, 1393.
295 D. Guo, R. Shibuya, C. Akiba, S. Saji, T. Kondo, J. Nakamura, *Science* **2016**, *351*, 361.
296 T. H. Lee, S. Y. Kim, H. W. Jang, *Nanomaterials* **2016**, *6*, 194.
297 Z. Sofer, D. Sedmidubský, S. Huber, J. Luxa, D. Bousă, C. Boothroyd, M. Pumera, *Angew. Chem., Int. Ed.* **2016**, *55*, 3382.
298 C. C. Mayorga-Martinez, Z. Sofer, M. Pumera, *Angew. Chem., Int. Ed.* **2015**, *54*, 14317.
299 H. Wu, X. Liu, J. Yin, J. Zhou, W. Guo, *Small* **2016**, *12*, 5276.
300 B. P. Bastakoti, Y. Sakka, K. C.-W. Wu, Y. Yamauchi, *J. Nanosci. Nanotechnol.* **2015**, *15*, 4747.
301 H.-Y. Lian, M. Hu, C.-H. Liu, Y. Yamauchi, K. C.-W. Wu, *Chem. Commun.* **2012**, *48*, 5151.
302 B. P. Bastakoti, Y. Kamachi, H.-S. Huang, L.-C. Chen,

K. C.-W. Wu, Y. Yamauchi, *Eur. J. Inorg. Chem.* **2013**, 39.
303 M. B. Zakaria, C. Li, Q. Ji, B. Jiang, S. Tominaka, Y. Ide, J. P. Hill, K. Ariga, Y. Yamauchi, *Angew. Chem., Int. Ed.* **2016**, *55*, 8426.
304 A. Wakamiya, S. Yamaguchi, *Bull. Chem. Soc. Jpn.* **2015**, *88*, 1357.
305 N. Aratani, A. Osuka, *Bull. Chem. Soc. Jpn.* **2015**, *88*, 1.
306 S. Yagai, *Bull. Chem. Soc. Jpn.* **2015**, *88*, 28.
307 Y. Tobe, K. Tahara, S. D. Feyter, *Bull. Chem. Soc. Jpn.* **2016**, *89*, 1277.
308 J. I. Paredes, S. Villar-Rodil, *Nanoscale* **2016**, *8*, 15389.
309 Y. Hernandez, V. Nicolosi, M. Lotya, F. M. Blighe, Z. Sun, S. De, I. T. McGovern, B. Holland, M. Byrne, Y. K. Gun'Ko, J. J. Boland, P. Niraj, G. Duesberg, S. Krishnamurthy, R. Goodhue, J. Hutchison, V. Scardaci, A. C. Ferrari, J. N. Coleman, *Nat. Nanotechnol.* **2008**, *3*, 563.
310 Z. Wang, W. Guan, Y. Sun, F. Dong, Y. Zhou, W.-K. Ho, *Nanoscale* **2015**, *7*, 2471.